[redacted]

NASA

MEMORANDUM

ALTITUDE PERFORMANCE OF A FULL-SCALE HIGH-TEMPERATURE TURBOJET ENGINE USING PENTABORANE FUEL AND HEF-2

By Joseph N. Sivo and John P. Wanhainen

Lewis Research Center
Cleveland, Ohio

NATIONAL AERONAUTICS AND SPACE ADMINISTRATION
WASHINGTON
January 1959

[redacted]

NATIONAL AERONAUTICS AND SPACE ADMINISTRATION

MEMORANDUM 12-31-58E

ALTITUDE **PERFORMANCE** OF A FULL-SCALE HIGH-TEMPERATURE TURBOJET ENGINE USING PENTABORANE FUEL AND HEF-2*

By Joseph N. Sivo and John P. Wanhainen

A turbojet engine operating at high turbine inlet temperatures was run on both pentaborane fuel and HEF-2 at a simulated altitude of 50,000 feet and a flight Mach number of 0.8. The engine speed and turbine inlet temperature were held constant during both fuel tests. To reduce the viscosity of boric oxide that deposited on engine parts, most of the engine parts in contact with the combustion products of the boron fuels were designed to operate at high temperatures.

Inspection of the engine after each boron fuel run revealed that the elevated operating temperature of the engine did in fact reduce oxide deposition to an acceptable level. During the HEF-2 run a 2.5-percent decrement in net thrust occurred because of internal engine performance losses, compared with a 7-percent loss in the pentaborane fuel run. Changes in the thermodynamic properties of the combustion products of boron fuels compared with hydrocarbon fuels contributed an additional 4- to 5-percent thrust decrement in the HEF-2 run and a 5.5-percent decrement in the pentaborane run. The net-thrust specific fuel consumption was reduced approximately 22 percent with pentaborane fuel and 10 percent with HEF-2 as compared with hydrocarbon fuel, despite the combustion efficiency and net-thrust losses that occurred with the boron fuels.

INTRODUCTION

As part of a continuing NASA research program on the feasibility of using fuels in the boron hydride family for extending the range and altitude of military aircraft, an investigation was conducted at the Lewis Research Center using boron-containing fuels in a full-scale high-temperature turbojet engine. In prior investigations the main problem associated with the use of these fuels was the engine performance loss due to boric oxide deposition on engine parts. The initial full-scale engine tests using pentaborane fuel were conducted at normal turbojet-operating temperatures and are reported in references 1 to 3.

*Title, Confidential.

Investigations into the physical properties of boric oxide reported in references 4 and 5 indicate that significant reductions in viscosity would be realized if the operating temperature of the engine were raised. It was felt that reductions in oxide deposits would accompany the viscosity reduction. This fact was borne out in part by work resorted in reference 6 on the effect of both turbine stator shape and blade operating temperature on oxide deposition. It was shown that increasing the blade temperature did significantly reduce the oxide deposits.

To evaluate the effect of an increase in engine operating temperature on full-scale engine performance, a J47 turbojet engine was modified with the cooperation of the engine manufacturer to include a high-temperature turbine wheel, a special stator assembly, and an NASA annular combustor designed specifically for use with boron hydride fuels. In the investigation reported herein engine performance was evaluated at one design point using both pentaborane fuel and HEF-2. The turbine inlet temperature was 2140° F for the pentaborane run and 1900° F for the HEF-2 run. The engine was operated in an altitude test chamber at a simulated altitude of 50,000 feet and a flight Mach number of 0.8. The data presented herein show component as well as over-all engine performance with operation on both fuels. Photographs of boric oxide deposits on major engine components are also included.

APPARATUS AND PROCEDURE

Engine

A schematic diagram of the engine used in this investigation is shown in figure 1. The engine was a modified 547 engine consisting of an axial-flow compressor, an annular combustor, and a single-stage turbine. The turbine rotor blades were of special high-temperature materials capable of operating at elevated temperatures. The turbine stator was not fabricated from the same material as the turbine rotor blades and therefore required stem-cooling at the maximum allowable turbine rotor temperatures. An afterburner tailpipe was used with a variable-area clamshell exhaust nozzle that permitted operation at the selected turbine outlet gas temperature and rated engine speed.

Combustor

A cross section of the NASA combustor, designed for use with boron hydride fuels and used in this investigation, is shown in figure 2. The liner walls were made up of a series of louvers arranged to produce a continuous film of air along the walls to minimize oxide deposition. A perforated plate was used at the combustor inlet to prevent a recirculation zone in the region of the fuel nozzles. Secondary-air mixing slots

were located approximately halfway down the combustor to control the combustor outlet temperature profiles. The combustor was similar to the one used in the investigations of references 1 and 7.

Details of the air-atomizing hydrocarbon fuel nozzle are shown in figure 3. Twenty of these nozzles, equally spaced circumferentially, provided radial injection of hydrocarbon fuel during engine checkout and operation prior to the boron fuel runs.

A sketch of the boron hydride fuel nozzles is shown in figure 4. These nozzles were also of the air-atomizing type. There were 40 fuel nozzles located to inject fuel axially, with 20 nozzles at each of two radial depths.

Fuel System

A dual fuel system was used that allowed operation with either boron fuel or hydrocarbon fuel, or both. The standard engine fuel system was used with hydrocarbon fuel. A diagram of the boron fuel system is shown in figure 5. Helium pressure was used to drive the boron fuel. Dry JP-4 fuel was used as a lead and purge liquid for the pentaborane fuel run; and, because of the incompatability of JP-4 with HEF-2, methyl toluene benzene was used as a lead and purge fuel in the HEF-2 run. The purge system used helium and purge liquid alternately to inert the system before and after each run.

The hydrocarbon fuel used was low-smoke, clear gasoline with a lower heating value of 18,971 Btu per pound. The pentaborane fuel used had a purity of 99 percent, and its properties were as follows:

Molecular weight	63.17
Melting point, °F	-52
Boiling point at 760 mm Hg, °F	136
Lower heating value, Btu/lb	29,100
Specific gravity at 32° F	0,644
Stoichiometric fuel-air ratio	0.0764
Pounds B_2O_3 per million Btu	94

The exact composition of the HEF-2 used was unknown; however, its approximate properties were as follows:

Molecular weight	105.25
Melting point, °F	-212
Boiling point at 760 mm Hg, °F	257
Lower heating value, Btu/lb	24,300
Specific gravity at 77° F	0.731
Stoichiometric fuel-air ratio	0.0726
Pounds B_2O_3 per million Btu	108

Instrumentation

The location of the instrumentation stations and the number of pressure and temperature instruments at each station are shown in figure 1. Thermocouples were located at the midchord and at the leading and trailing edges of several turbine stator blades to give an indication of the metal operating temperature. Thermocouples were also located at several radial positions on several turbine rotor blades. Engine airflow was measured at station 1. The fuel flow was measured with rotating-vane flowmeters in both fuel systems. Engine jet thrust was measured with a null-type thrust cell.

Installation

The engine was installed in an altitude test chamber consisting of a tank 10 feet in diameter and 60 feet long divided into two compartments by a bulkhead. Air at ram pressure was ducted from the front compartment to the engine inlet through a bellmouth inlet and a Venturi that was used to measure airflow. A labyrinth seal around the inlet duct was used to prevent leakage from the front to the rear compartment where the ambient altitude pressure was maintained. The engine was mounted on a thrust-measuring platform in the rear compartment.

Procedure

Before both boron hydride fuel runs the engine was operated on the hydrocarbon fuel to obtain engine performance data. During hydrocarbon operation fuel was fed through both fuel systems, approximately one-third of the total flow passing through the boron fuel system and nozzles. This was done to improve the combustor outlet temperature profiles, The switchover procedure in both boron fuel runs was the same: an immediate change from lead fuel to boron fuel in the boron fuel system followed by gradually decreasing the primary hydrocarbon fuel flow and increasing the boron fuel flow until the engine was operating solely on boron fuel.

For each run the exhaust-nozzle area and engine fuel flow were manually adjusted to maintain constant engine speed and exhaust-gas temperature. The engine was operated at a simulated altitude of 50,000 feet and a flight Mach number of 0.8. The nominal engine inlet temperature was 60° F. The engine speed was held at rated mechanical speed.

In the pentaborane fuel test the average turbine inlet temperature was 2140° F. At this temperature level the turbine stators required steam-cooling. As a result of uneven cooling, the maximum allowable local stator blade temperature of 2000° F was attained on only a few

stators, and the average blade temperature was below 1000° F. The pentaborane run lasted a total of 8 minutes, during 2 minutes of which the engine operated on a mixture of pentaborane and hydrocarbon fuels. The run was abruptly terminated by the occurrence of compressor stall. Engine performance data were recorded throughout the run.

In the HEF-2 test, the engine was temperature-derated to an average turbine inlet gas temperature of 1900° F. At this temperature the stator was run uncooled with a maximum local blade temperature of 2000° F and an average blade temperature of 1700° F. The run lasted approximately 9 minutes, about 3.4 minutes of which the engine operated on a mixture of HEF-2 and hydrocarbon fuel. The run was terminated when one of the boron fuel nozzles plugged during the run, causing a local hot spot that resulted in failure of a turbine stator blade. Performance data were taken throughout the run.

To eliminate the effects of minor changes in the actual operating point and thus better show the performance trends in both boron fuel runs, the data presented herein have been adjusted to a fixed operating point for each run. The fixed operating point chosen for each run agreed closely with the actual operating point. The symbols used herein are listed in appendix A, and the methods of calculation are presented in appendix B.

RESULTS AND DISCUSSION

Oxide Formation and Deposition

One of the products of combustion of boron compounds is boric oxide, which is a viscous fluid at the temperatures generally encountered in turbojet engines. If thermal decomposition of the boron fuel occurs before complete combustion, the product of decomposition tends to form clinkers similar to coke formations with hydrocarbon fuels. The 131 pounds of pentaborane fuel used formed approximately 358 pounds of boric oxide. The 120 pounds of HEF-2 used formed approximately 315 pounds of boric oxide. The weights of oxide formed were determined by calculation from fuel-flow measurements. The major portions of this oxide passed through the engine in the form of microscopic drops of liquid suspended in the main gas stream. However, some oxide was deposited on the metal surfaces that were in contact with the boric-oxide-containing gas stream. There was little evidence of decomposed fuel in the oxide deposits. The weights of the oxide deposits on the engine parts were not determined.

Examination of the combustor section following each run showed that the boron fuel nozzles remained completely free of oxide deposits. The combustor walls were relatively free of oxide deposits, as shown in figure 6. This photograph was made after the HEF-2 run but is typical

of the combustor appearance after both runs. The major difference between the two fuel runs other than the fuels themselves was the average operating turbine stator blade temperatures. In the pentaborane run the operating gas temperature was the higher of the two runs, but as a result of the required stator blade cooling the average blade temperature was below 1000° F. In the HEF-2 run the stator blades were uncooled and the average blade temperature was 1700° F.

The results of these differences in stator blade temperatures are shown in figures 7 and 8. The pentaborane fuel run resulted in generally heavy boric oxide deposits on the stator blades. However, in the area where the stator blades operated near limiting temperature (fig. 7(b)), there was little oxide deposit on the blades. In the REF-2 run the elevated stator blade temperatures resulted in marked reduction in oxide deposits on the stator blades (fig. 8). The blades were rather uniformly coated with a thin film of oxide that had apparently reached an equilibrium thickness. In both tests the turbine rotor was very clean, with only a very thin glassy coating of oxide on the blades (figs. 7(c) and 8(d)). The combination of high rotor blade metal temperatures and high centrifugal forces exerted on the oxide that reaches the blades is responsible for the clean rotor.

Photographs of the oxide deposits on the engine tailpipe and tailpipe diffuser are shown in figures 9(a) and (b) for the pentaborane run and in figures 9(c) and (d) for the REF-2 run. Most of the tailpipe and diffuser surfaces had a very thin coating of glassy boric oxide that appeared to have reached an equilibrium thickness. In the vicinity of the turbine, the oxide deposits were very rough and hence appear thick. Motion pictures of the boric oxide flow on the tailpipe walls at the turbine discharge were taken through a window in the tailpipe during the pentaborane run. The movies, although limited in scope, did indicate that the surface roughness and also a large portion of the indicated oxide deposits in this region occurred during the shutdown period when decreasing temperatures resulted in marked increases in oxide viscosity. The exhaust nozzle was free of oxide deposits that could affect nozzle flow area, as shown in figures 9(b) and (d), but some difficulty was encountered in nozzle operation during the runs as a result of oxide deposits at the nozzle pivot points.

Effects of Boric Oxide Deposits on Component Performance

The combustion efficiencies for the pentaborane fuel and the REF-2 runs are shown in figure 10(a). The scatter in the data points reflects the difficulty encountered in setting a steady-state point in the time available for the runs. At reasonably steady-state conditions the pentaborane efficiency was approximately 86 percent and that of REF-2 was

approximately 90 percent. The low efficiencies obtained reflect the emphasis the fuel-nozzle design placed on oxide-free combustor operation rather than on maximum obtainable efficiency. It is felt that, with sufficient development effort, a fuel nozzle capable of oxide-free operation at high efficiency is possible.

The combustor total-pressure loss is shown in figure 10(b) for both runs. The fact that there was no increase in total-pressure loss during the tests indicates an oxide-free combustor.

The turbine efficiencies for both fuel runs are shown in figure 11(a). In the pentaborane run, turbine efficiency decreased rapidly from 0.70 to 0.635 during the run. This decrease is a direct reflection of the effects of heavy oxide deposits on the stator blades. On the other hand, the turbine efficiency in the HEF-2 run remained essentially constant throughout the run.

The effect of the accumulation of oxide deposits on the stator blades is graphically shown in figure 11(b), where the calculated stator flow area is shown for each run. As expected, there was a marked decrease in flow area of approximately 10 percent in the pentaborane run and essentially no change in flow area during the HEF-2 run.

The turbine total-temperature ratio (fig, 11(c)) increased about 1 percent during the pentaborane run, mainly as a result of increased work requirements. Temperature ratio increased slightly during the HEF-2 run as a result of gas-property changes.

The turbine total-pressure ratio for the pentaborane fuel run increased 17 percent over that for operation with gasoline (fig. 11(d)). This was primarily a result of increased pressure loss through the stators plus increased work requirements and the change in thermodynamic properties of the working fluid. In the HEF-2 run the increase in pressure ratio was primarily a result of thermodynamic property changes in the working fluid.

Decreases in turbine performance, whether increased pressure drop due to oxide deposits or decreased efficiency of the turbine rotor, combine with the changes in thermodynamic properties of the working fluid to increase the turbine outlet Mach number. The effect of boron fuel operation on turbine outlet Mach number (i.e., tailpipe inlet Mach number) is shown in figure 12 for both fuel runs. In both cases the Mach number increased above that with gasoline. In the pentaborane run, the increase was from 0.47 to 0.56, or approximately 0.1 Mach number. In the HEF-2 run, the change in Mach number was 0.05. Although in the pentaborane fuel run the marked decrease in turbine performance did result in an increase in the turbine outlet Mach number, the increase was small in

comparison with that reported in reference 1, where very large changes in turbine outlet Mach number occurred. The turbine performance loss reported in reference 1 was only half that reported herein. However, because of the higher initial turbine outlet Mach number in reference 1, the effect of the turbine performance loss on Mach number was magnified.

Increases in Mach number are reflected in increased tailpipe total-pressure losses. Tailpipe total-pressure loss is plotted against time for both boron fuel runs in figure 13(a). In the pentaborane run the loss increased from 6.4 to 9.0 percent, and in the HEF-2 run the loss increased from 7.4 to 9.2 percent. The increased losses in both runs are primarily a result of Mach number increases and not increased drag coefficient due to oxide buildup. To illustrate the dependence of tailpipe losses on Mach number, the pressure-loss data from all runs including the gasoline calibration data are generalized as a function of Mach number in figure 13(b).

Effect of Oxide Deposition on Over-All Performance

The decreases in internal engine performance plus the change in thermodynamic properties of the working fluid are reflected in a decrease in engine total-pressure ratio at a constant engine temperature ratio, The effect of internal performance loss, excluding tailpipe loss, on engine pressure ratio is presented in figure 14. In the pentaborane run the pressure ratio decreased 9.5 percent. Of this decrease, approximately 5.5 percent was a result of internal engine performance losses. In the HEF-2 run the 5.5-percent decrease in pressure ratio was primarily due to thermodynamic property changes and is not a result of engine performance losses.

Engine corrected airflow is plotted against time in figure 15 for both fuel runs. In the pentaborane run corrected airflow decreased 2 percent. The oxide buildup on the turbine stator blades caused a shift in the operating point of the compressor that resulted in the decreased airflow. In the HEF-2 run no apparent change in airflow was noted.

The over-all engine net thrust is presented in figure 16(a) in terms of percent of the thrust obtained with gasoline fuel for both runs. It must be remembered that a direct comparison with gasoline operation includes performance changes resulting from the gas-property changes in the combustion products of the two fuels. During the pentaborane run the net thrust decreased a total of 12.5 percent. In the HEF-2 run the decrease was only 7.5 percent.

To give a better insight as to the reasons for the thrust loss, a breakdown of the factors contributing to the losses is presented in figures 16(b) and (c) for the pentaborane and HEF-2 runs, respectively.

In the pentaborane run (fig. 16(b)) the thrust loss due to the change in thermodynamic properties of the working fluid amounted to 5.3 percent. The loss due to internal engine losses was an additional 5.7 percent. This was primarily due to turbine performance losses. Tailpipe losses added another 1.5 percent. In the HEF-2 run (fig. 16(c)) the initial loss due to thermodynamic property changes was 4 to 5 percent. Approximately 1 percent additional loss was due to internal performance losses, and 1.5 percent due to tailpipe pressure losses.

Although, to this point, only decreases in engine performance with boron fuel operation have been cited, the over-all performance picture as it affects the all-important net-thrust specific fuel consumption indicates a substantial net gain compared with gasoline fuel. In the pentaborane run a net improvement of 22 percent in specific fuel consumption was realized. With the lower-energy-containing HEF-2, a net improvement of 10 percent in specific fuel consumption was noted.

In comparing the percentage improvements in specific fuel consumption for the two fuels, it must be kept in mind that the lower heating value of HEF-2 permits only about half the theoretical improvement attainable with pentaborane fuel. Thus, of course, the fractional gains in specific fuel consumption obtainable with KEF-2 are twice as sensitive to incremental engine performance changes as with pentaborane fuel.

The results of the HEF-2 test did, to a large measure, fulfill the hope that increasing the operating temperature of all engine parts in contact with the boric oxide would reduce the oxide deposition to an acceptable level. Even in the pentaborane run, with the exception of the cool turbine stator blades, the advantages of high temperatures were clearly illustrated. With proper design of all engine parts in conjunction with moderately high operating temperatures, very nearly all the theoretical gains in engine performance (i.e., specific fuel consumption improvements) can be realized from boron-containing fuels.

SUMMARY OF RESULTS

A turbojet engine operating at moderately high turbine inlet temperatures was run with pentaborane fuel and REF-2. Inspection of the engine after each fuel run revealed that, with the exception of the turbine stators in the pentaborane run, there was very little boric oxide accumulation on engine parts. From the nature and thickness of the oxide deposition that did occur, it appeared that an equilibrium thickness had been reached. Thus, the higher operating temperatures were proved to be beneficial in reducing the oxide buildup on the turbine assembly that would eventually lead to deterioration of its performance.

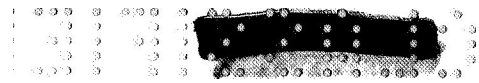

During the HEF-2 run, where boric oxide deposition was at a minimum, there was only a 2.5-percent reduction in net thrust due to reductions in turbine performance and increased tailpipe pressure losses. This loss is compared with a 7-percent net-thrust decrement during the pentaborane fuel run. In both fuel runs approximately a 1.5-percent loss in net thrust occurred because of increased tailpipe pressure losses. Thus, only a 1-percent decrement in thrust occurred in the HEF-2 run as a result of turbine performance loss, compared with 5.5 percent that occurred in the pentaborane runs. The thermodynamic property changes in the combustion products of boron fuels as compared with those of hydrocarbon fuels contributed an additional 4- to 5-percent thrust decrement for the HEF-2 run and a 5.5-percent decrement for the pentaborane run.

Although losses occurred in both net thrust and combustion efficiency (approx. 5 percent in both runs) during engine operation with boron fuels, there was a net gain of 22 percent in net-thrust specific fuel consumption with pentaborane fuel and a 10-percent gain with the lower-energy HEF-2. It must be remembered that, because of its lower energy content, HEF-2 offers only half the theoretical improvement in specific fuel consumption possible with pentaborane fuel.

Lewis Research Center
National Aeronautics and Space Administration
Cleveland, Ohio, September 24, 1958

APPENDIX A

SYMBOLS

A	area, sq ft
C_v	velocity coefficient
F_j	jet thrust, lb
F_n	net thrust, lb
F_s	thrust-system scale reading, lb
g	acceleration due to gravity, ft/sec^2
P	total pressure, lb/sq ft
P	static pressure, lb/sq ft
R	gas constant, ft-lb/(lb)(^oR)
T	total temperature, ^oR
V	velocity, ft/sec
w	weight flow, lb/sec
γ	ratio of specific heats
δ	ratio of total pressure to NASA standard sea-level pressure of 2116 lb/sq ft
η	efficiency
θ	ratio of total temperature to NASA standard sea-Level temperature of 518.7° R
φ	flow coefficient

Subscripts:

a	air
ac	actual
at	atomizing

B	combustor
Cl	compressor seal leakage
cc	camera cooling
f	fuel
i	vena contracta at exhaust-nozzle outlet
id	ideal
sl	seal
T	turbine
Tc	turbine cooling
t	total
0	free stream
1	airflow measuring station
2	compressor inlet
3	compressor outlet
4	turbine inlet
5	turbine outlet
9	exhaust-nozzle inlet
10	exhaust-nozzle discharge

APPENDIX B

METHODS OF CALCULATION

Airflow

Engine inlet airflow was calculated from measurements at station 1 by use of the following equation:

$$w_{a,1} = \varphi A_1 p_1 \sqrt{\frac{g}{RT_1}} \sqrt{\frac{2\gamma_1}{\gamma_1 - 1} \left(\frac{P}{p}\right)^{\frac{\gamma_1 - 1}{\gamma_1}} \left[\left(\frac{P}{p}\right)^{\frac{\gamma_1 - 1}{\gamma_1}} - 1\right]}$$

A flow coefficient φ of 0.994 was used and is defined as the ratio of the actual flow to the airflow computed on the basis of one-dimensional flow by use of free-stream total pressures and the static pressure in the Venturi throat.

Compressor leakage, turbine cooling, atomizing, and camera cooling airflows were calculated from total pressures, total temperatures, and static pressure in the same manner as engine airflow. The airflows and gas flows at the various stations throughout the engine were calculated as follows:

$$w_{a,2} = w_{a,1}$$

$$w_{a,3} = w_{a,2} - w_{a,Cl}$$

$$w_{a,4} = w_{a,3} + w_{a,at}$$

$$w_{a,5} = w_{a,4}$$

$$w_{a,9} = w_{a,2} - w_{a,Cl} + w_{a,at} + w_{a,cc} + w_{a,Tc}$$

$$w_{t,4} = w_{a,4} + w_f$$

$$w_{t,9} = w_{a,9} + w_f$$

[redacted]

Thrust

The over-all jet thrust determined from the thrust-system measurements was calculated from the following equation:

$$F_j = F_s + A_{sl}(p_1 - p_{10})$$

where A_{sl} is the area of the seal around the engine inlet.

The net thrust was determined by subtracting the inlet momentum from the jet thrust:

$$F_n = F_j - \frac{w_{a,1} V_0}{g}$$

The calculated jet thrust used in determining the breakdown of thrust loss was obtained from the following equation:

$$F_{j,5} = \left[\frac{w_{t,5}}{g} V_i + A_i(p_i - p_0)\right] C_V$$

The calculation was made using the measured values of pressure, temperature, and mass flow at the turbine outlet. A value for the velocity coefficient C_V of 0.95 was determined for the exhaust nozzle from a ratio of measured jet thrust to calculated jet thrust at the exhaust nozzle.

Combustian Efficiency

Combustion efficiency is defined as the ratio of ideal engine fuel flow to actual engine fuel flow:

$$\eta_B = \frac{w_{f,id}}{w_{f,ac}}$$

The ideal fuel flow is defined as the fuel flow required to satisfy a heat balance across the engine using the measured temperatures and an ideal combustion process. Fuel flows associated with ideal combustion processes were obtained from unpublished data.

[redacted]

Combustor Outlet Temperature

A heat balance across the combustor using the ideal engine fuel flow and the combustor inlet temperature was made to calculate combustor outlet temperature. The temperature rise associated with an ideal fuel flow was obtained from unpublished data.

Turbine Efficiency

Turbine efficiency was calculated from the following equation:

$$\eta_T = \frac{1 - \frac{T_5}{T_4}}{1 - \left(\frac{P_5}{P_4}\right)^{\frac{\gamma-1}{\gamma}}}$$

Area

Turbine stator area and exhaust-nozzle area were calculated as follows:

$$A = \frac{w_t \sqrt{\frac{RT}{g}}}{p\sqrt{\frac{2\gamma}{\gamma - 1}\left(\frac{P}{p}\right)^{\frac{\gamma-1}{\gamma}}\left[\left(\frac{P}{p}\right)^{\frac{\gamma-1}{\gamma}} - 1\right]}}$$

where P/p is considered critical.

Turbine Outlet Mach Number

The turbine-outlet Mach number was calculated from flow continuity using the mass flow, total temperature, total pressure, and area at the turbine outlet.

REFERENCES

1. Sivo, Joseph N.: Altitude Performance of a Turbojet Engine Using Pentaborane Fuel. NACA RM E57C20, 1957.

2. Useller, James W., Kaufman, Warner B., and Jones, William L.: Altitude Performance of a Full-Scale Turbojet Engine Using Pentaborane Fuels, NACA RM E54K09, 1957.

3. Useller, James W., and Jones, William L.: Extended Operation of Turbojet Engine with Pentaborane. NACA RM E55L29, 1957.

4. Setze, Paul C.: A Review of the Physical and Thermodynamic Properties of Boric Oxide. NACA RM E57B14, 1957.

5. Setze, Paul C.: A Theoretical and Experimental Study of Boric Oxide Deposition on a Surface Immersed in an Exhaust Gas Stream from a Jet-Engine Combustor, Including a Method of Calculating Deposition Rates on Surfaces, NACA RM E57F18, 1957.

6. Setze, Paul C., and Nusbaum, William J.: A Preliminary Study of the Effects of Boric Oxide Deposits on the Performance of Two Selected Turbine Stator-Blade Shapes. NACA RM E57L18, 1958.

7. Kaufman, Warner E., Lezberg, Erwin A., and Breitwieser, Roland: Preliminary Evaluation of Pentaborane in a 1/4-Sector of an Experimental Annular Combustor. NACA RM E56B13, 1957.

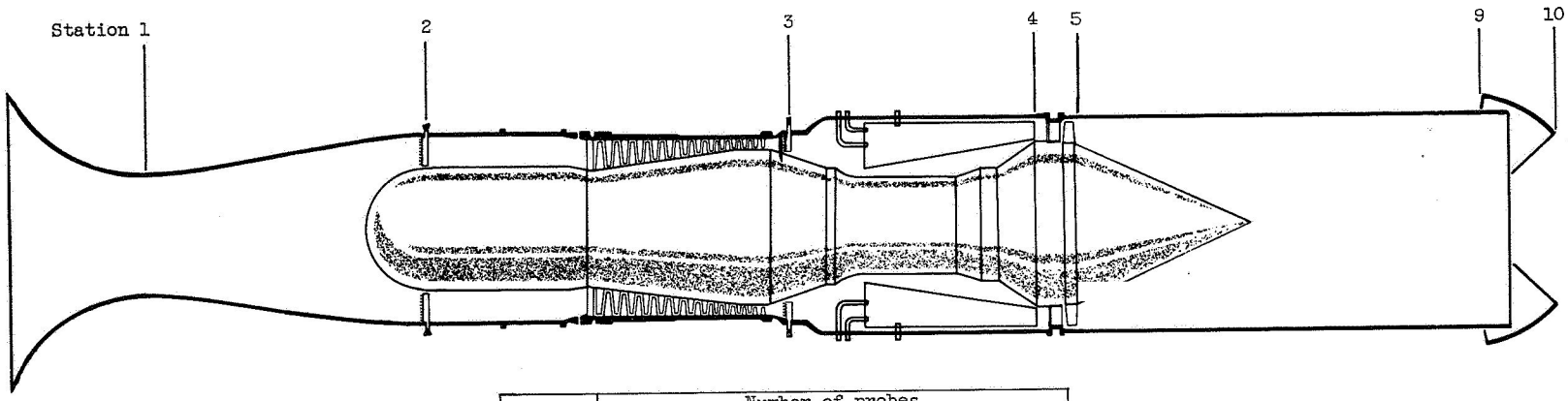

Station	Number of probes		
	Static pressure	Total pressure	Total temperature
1	4	4	--
2	--	5 Individual probes 3 Averaging rakes	10
3	--	15	10
4	--	4	--
5	4	20	33
9		24	24
10	4	--	--

CD-6343

Figure 1. - Schematic sketch of engine showing station locations.

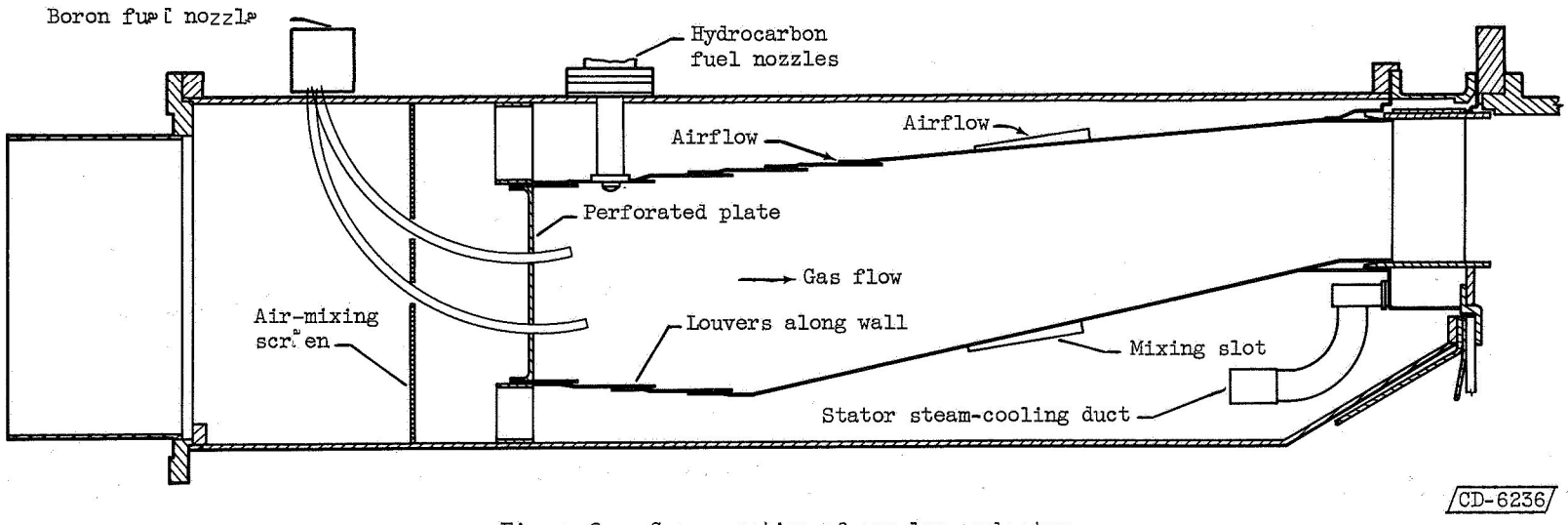

Figure 2. - Cross section of annular combustor.

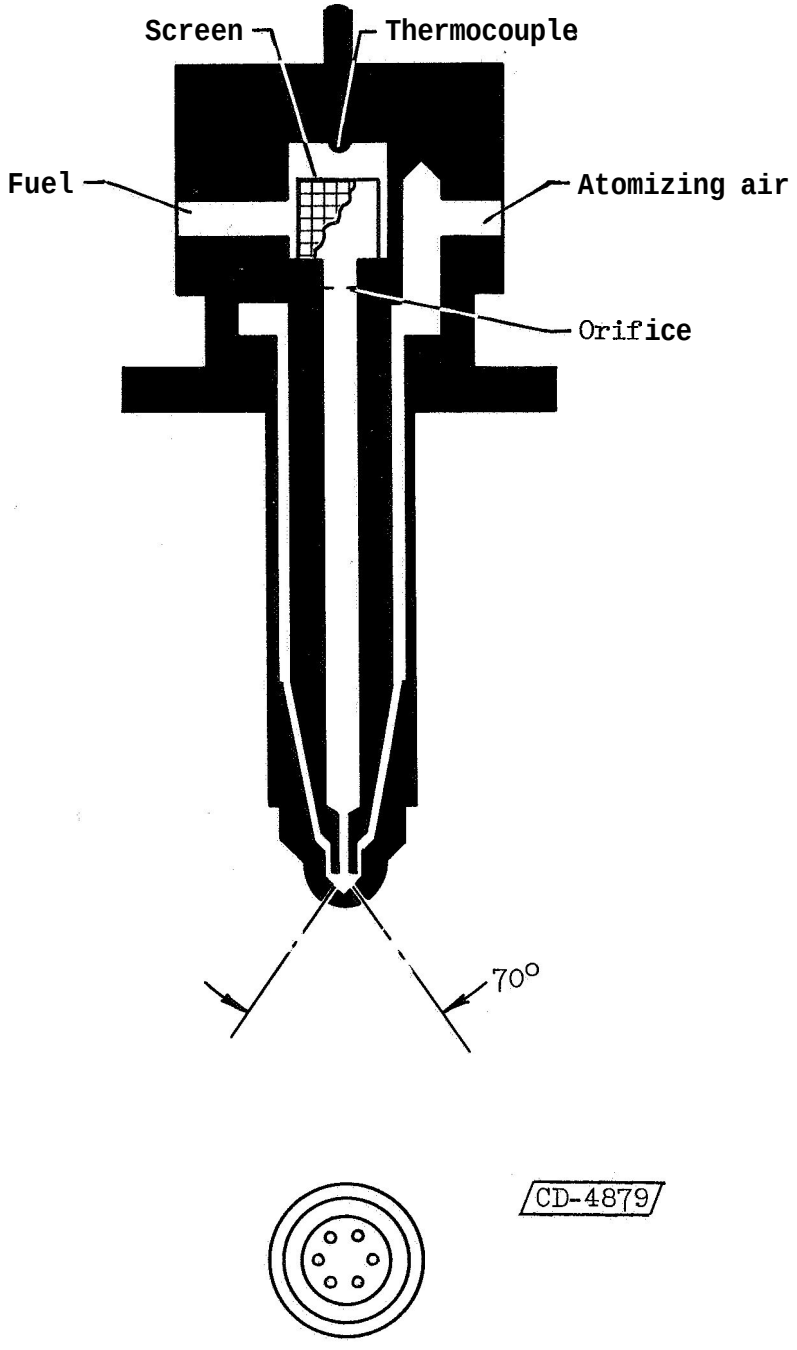

Figure 3. - Hydrocarbon-fuel nozzle assembly.

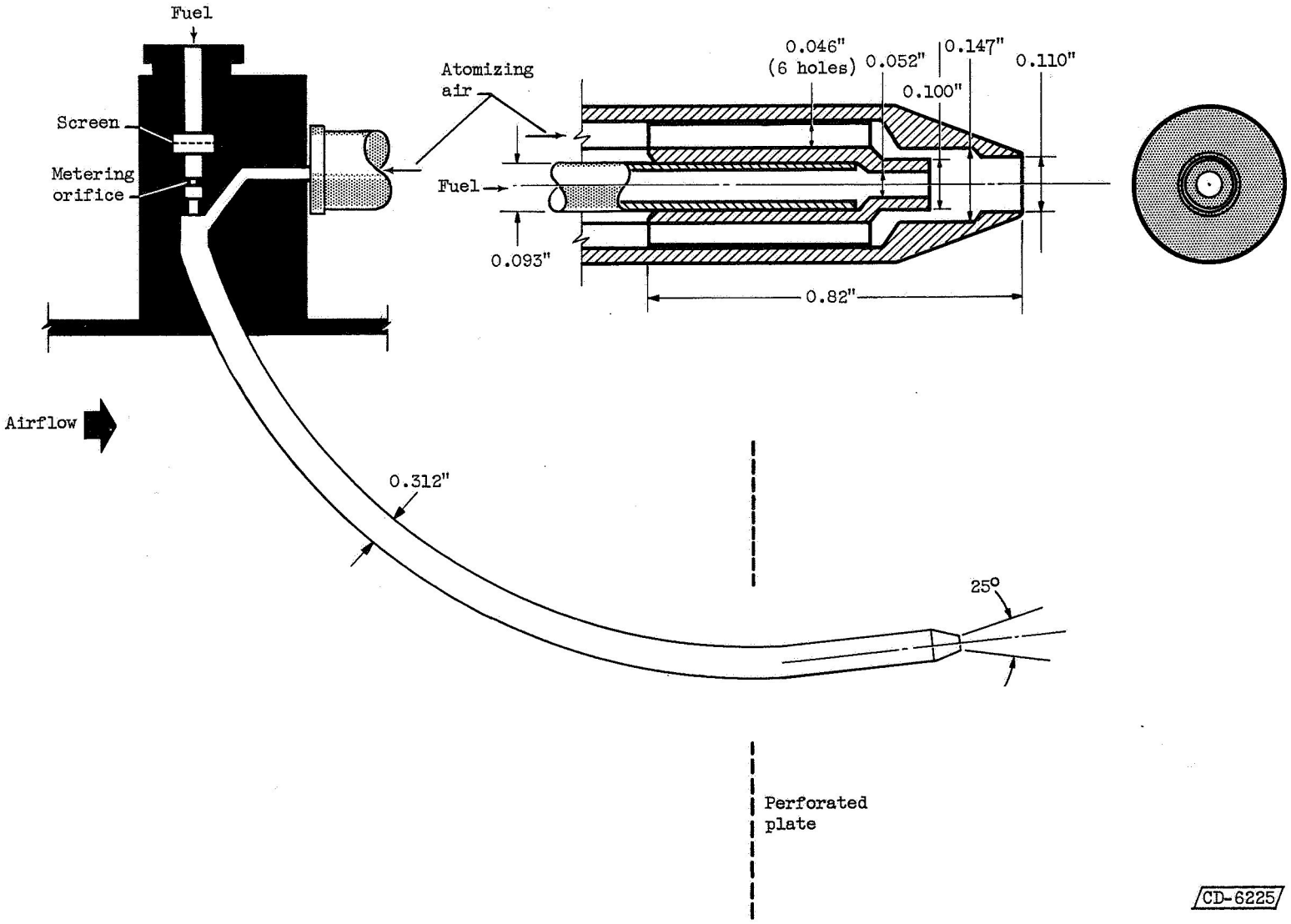

Figure 4. - Schematic diagram of boron fuel nozzle.

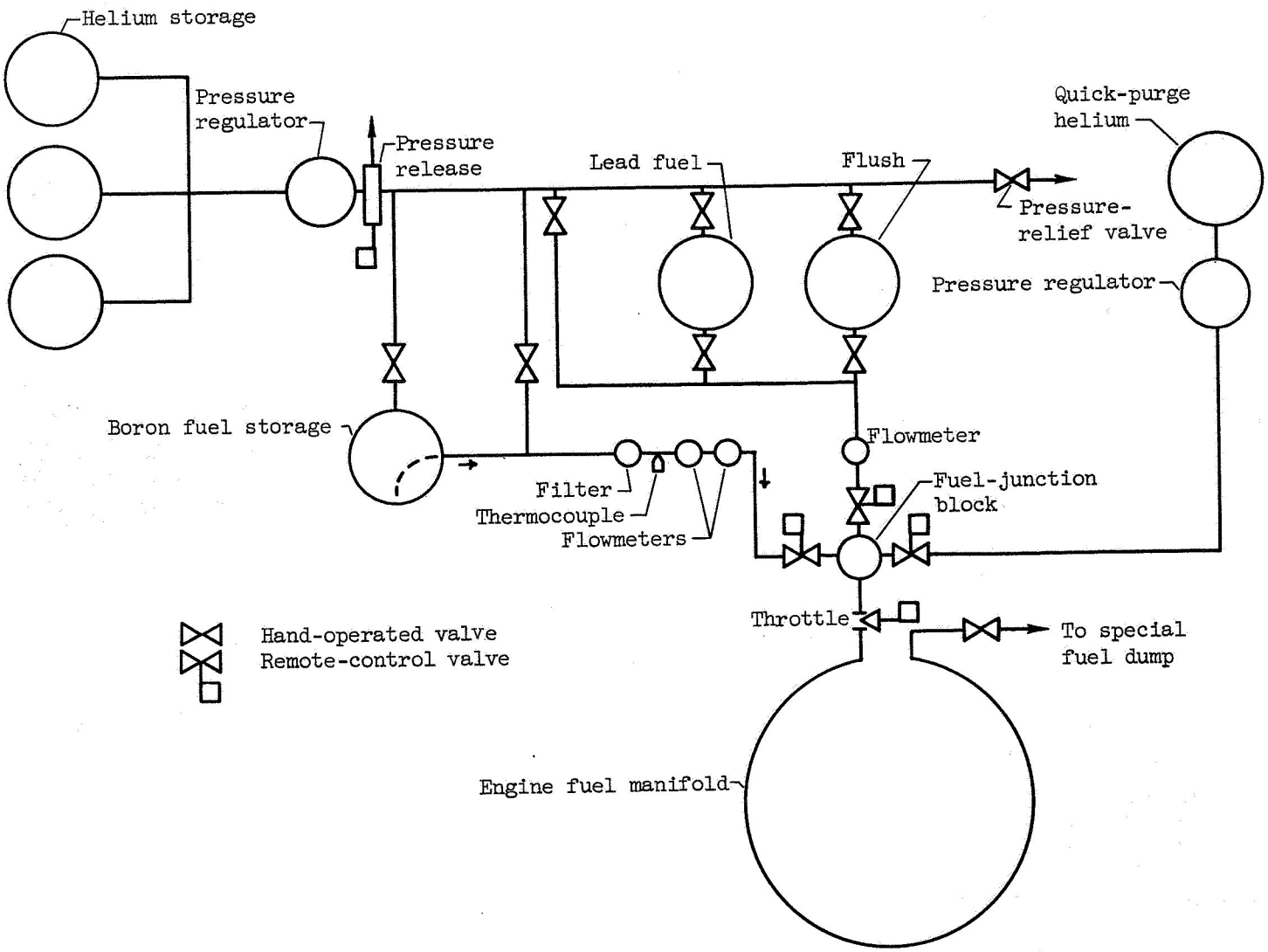

Figure 5. - Diagram of boron fuel system.

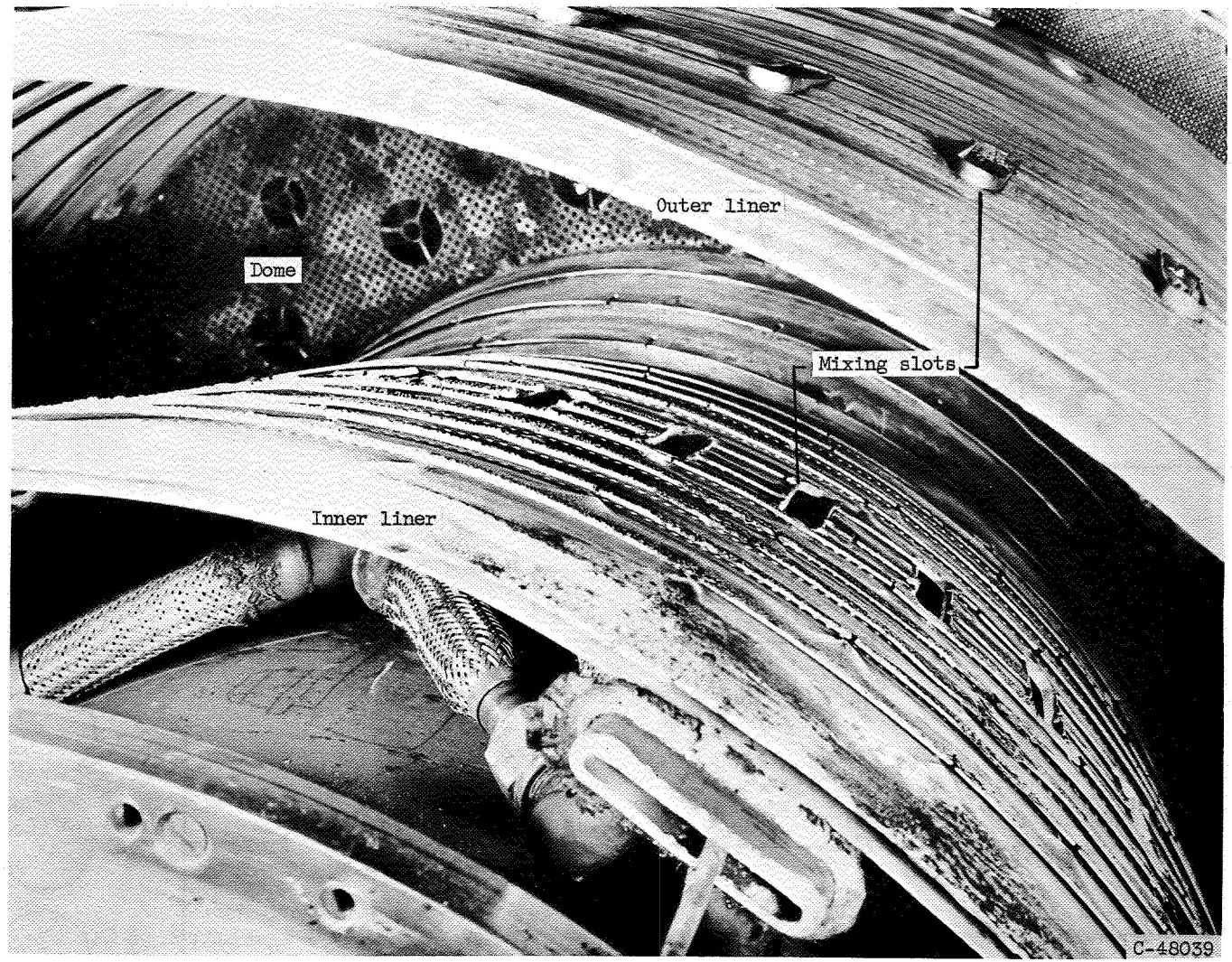

Figure 6. - Oxide deposits on combustor parts after HEF-2 run, looking upstream with stator assembly removed from engine.

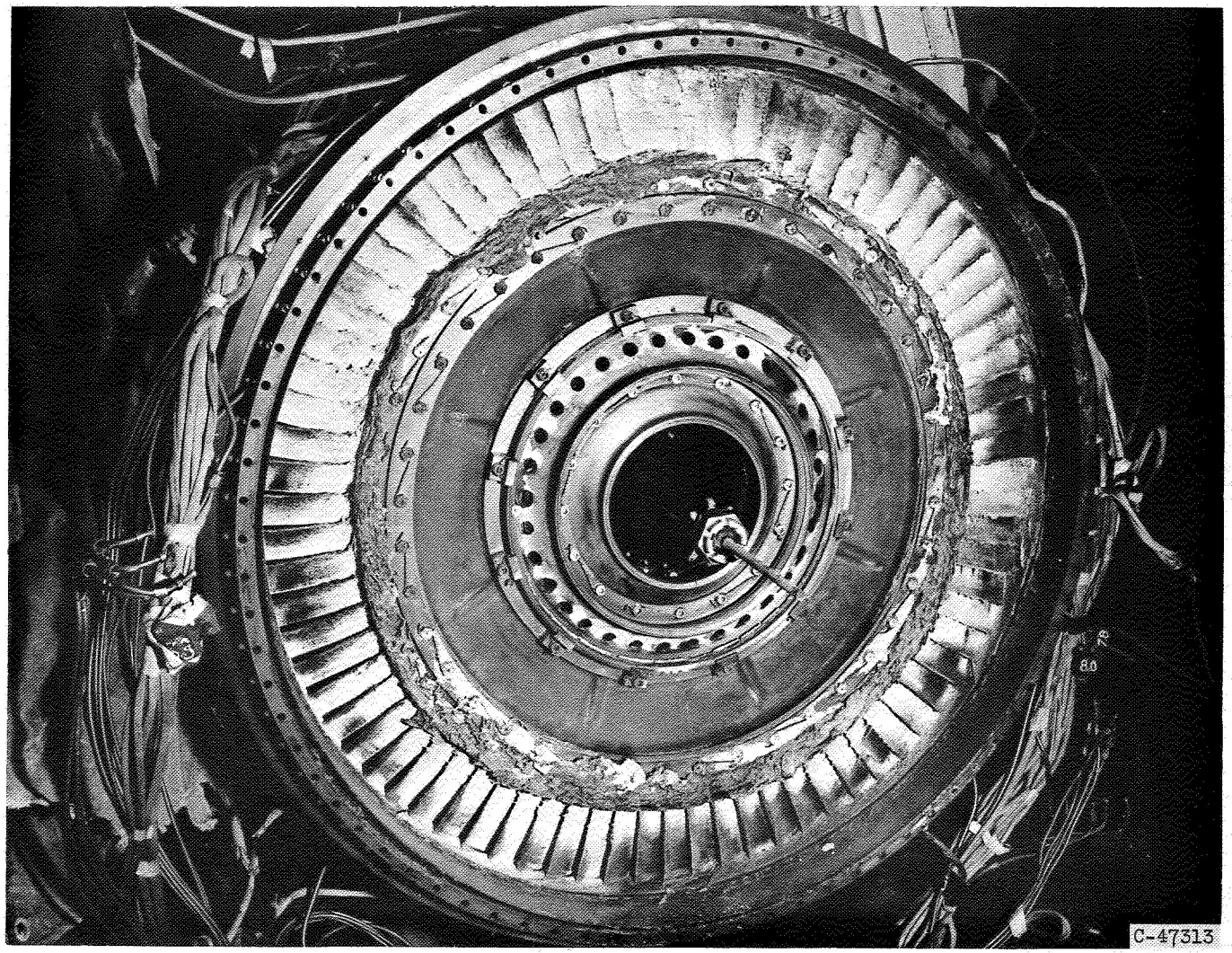

(a) Turbine stator, full view of downstream face

Figure 7. - Oxide deposits on turbine parts after pentaborane run.

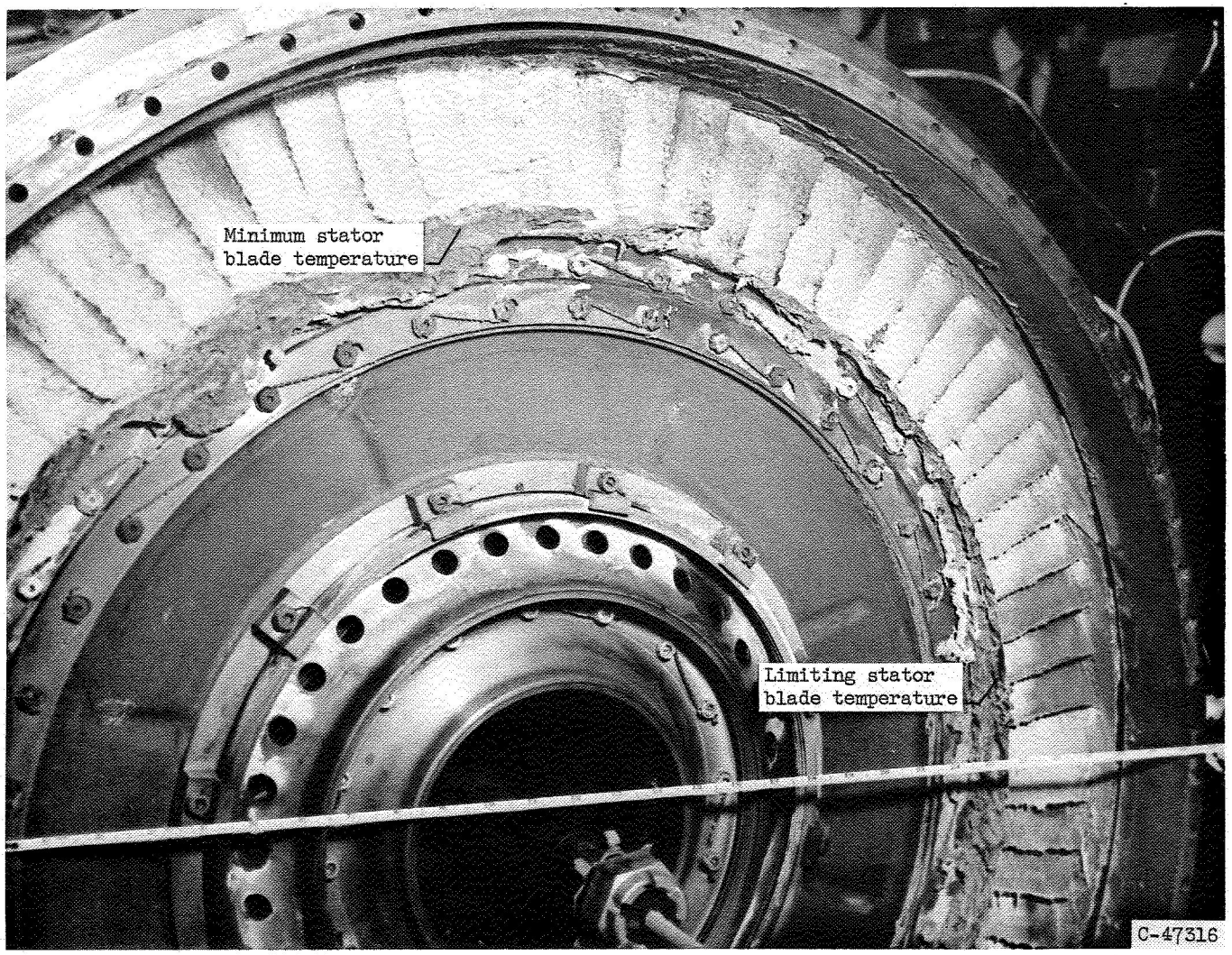

(b) Turbine stator, closeup view of aft stream face.

Figure 7 - Continued. Oxide deposits on turbine parts after pentaborane run.

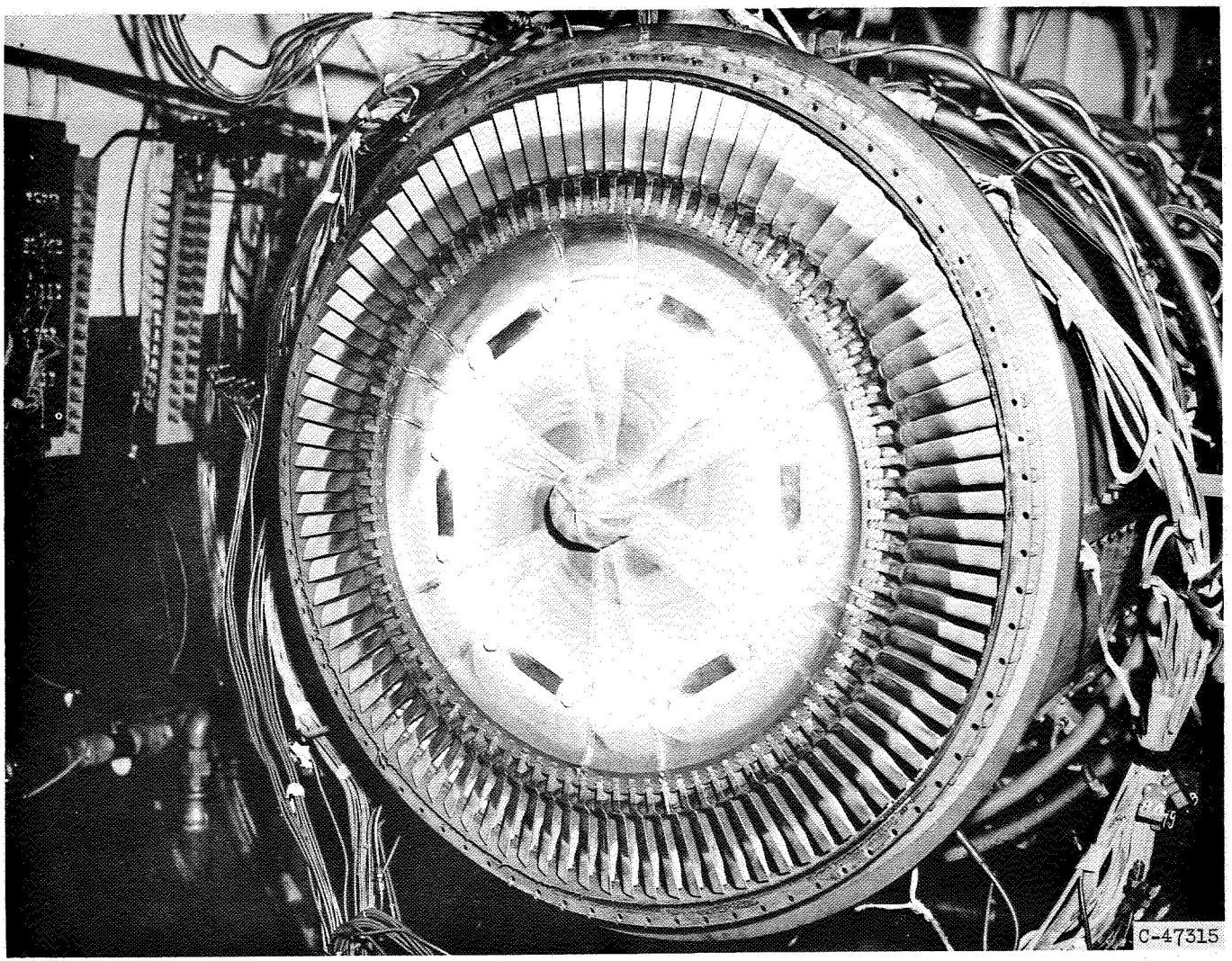

(c) Turbine rotor.

Figure 7 - Concluded. Oxide deposits on turbine parts after pentaborane run.

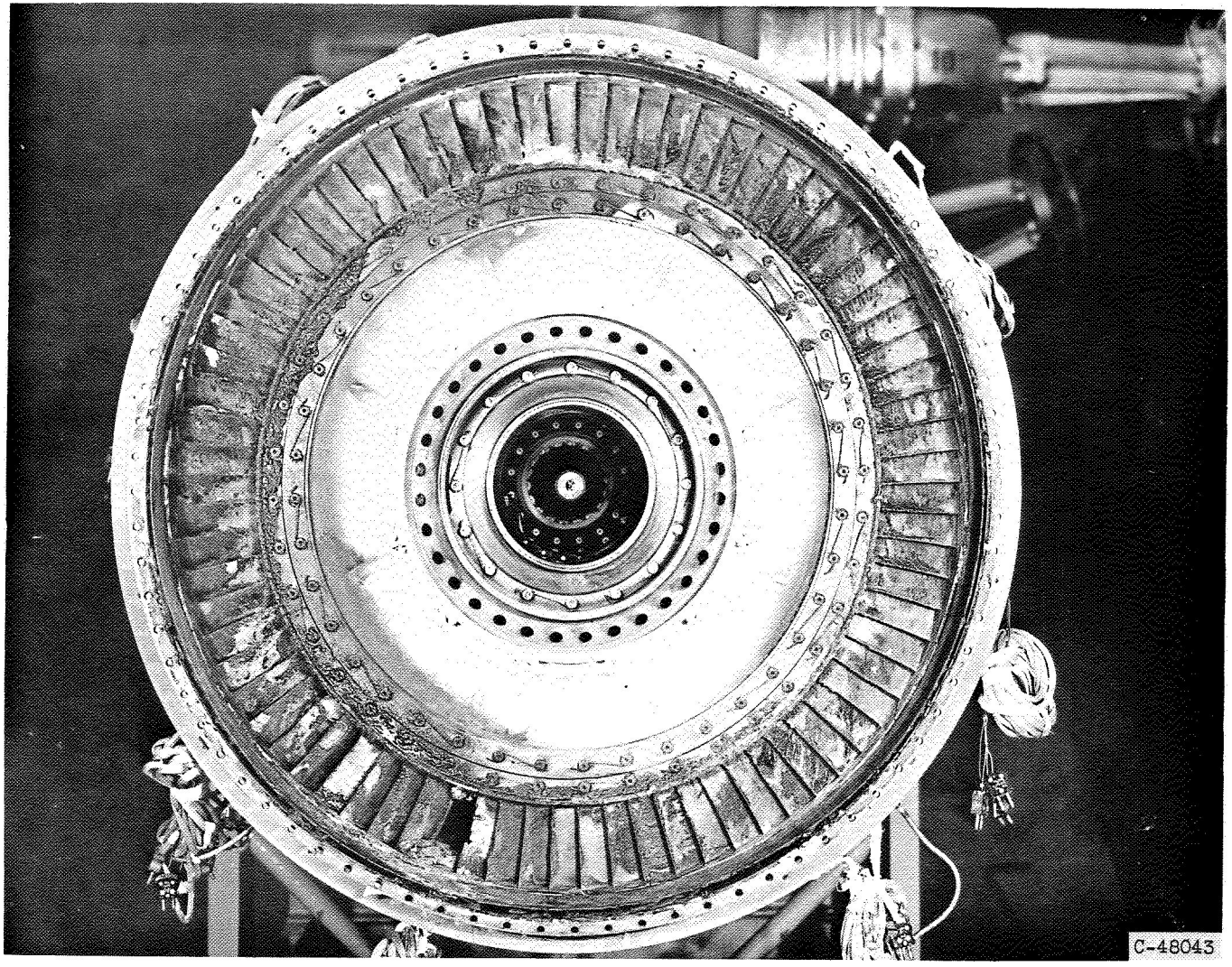

(a) Turbine stator, full view of downstream face.

Figure 8. - Oxide deposits on turbine parts after HEF-2 run.

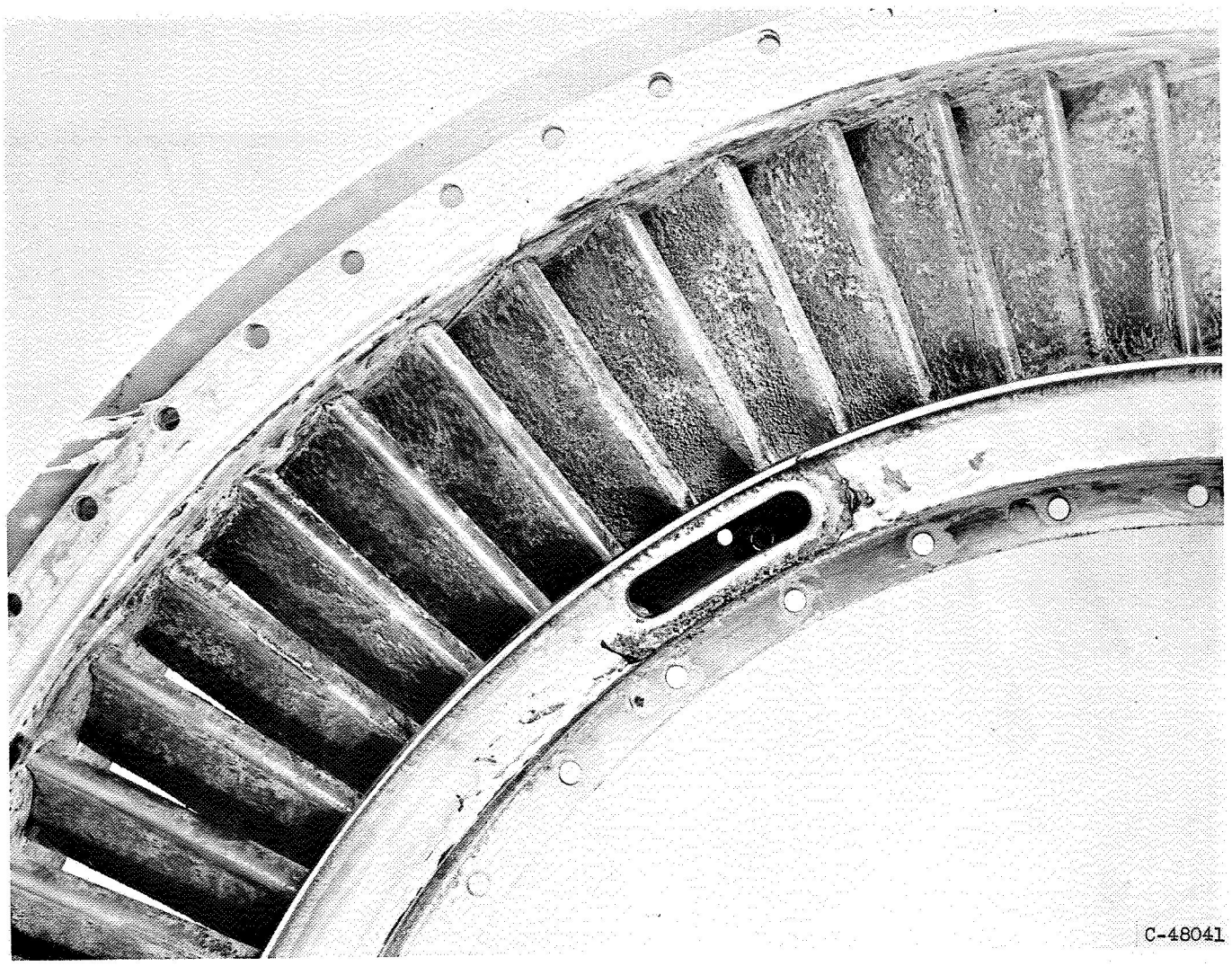

(b) Turbine stator, upstream-face pressure surface

Figure 8. - Continued. Oxide deposits on turbine parts after HEF-2 run.

(c) Turbine stator, upstream-face suction surface.

Figure 8. - Continued. Oxide deposits on turbine parts after HEF-2 run.

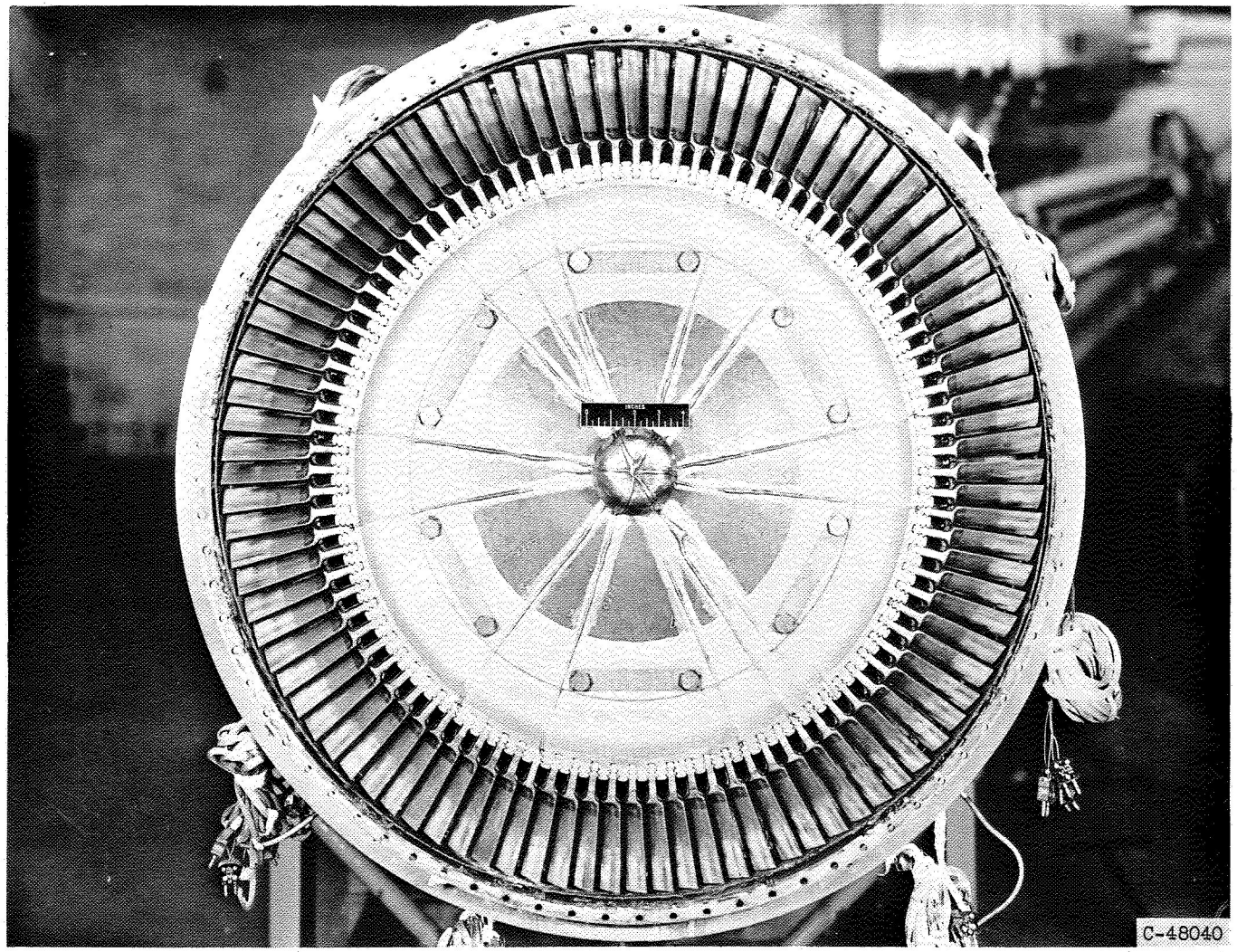

(d) Turbine rotor.

Figure 8. - Concluded. Oxide deposits on turbine parts after HEF-2 run.

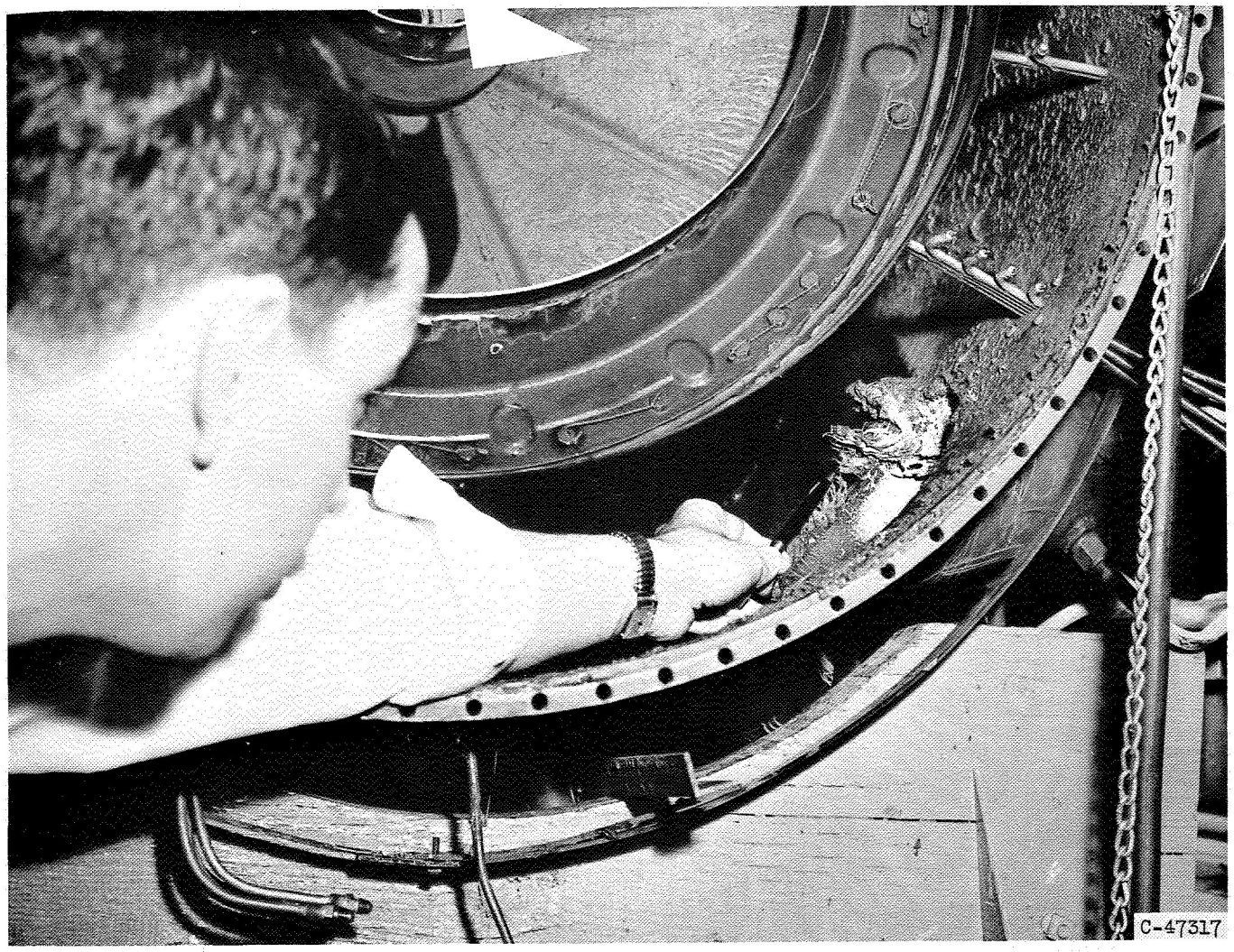

(a) Tailpipe, pentaborane run.

Figure 9. - Oxide deposits on tailpipe diffuser, tailpipe, and exhaust nozzle.

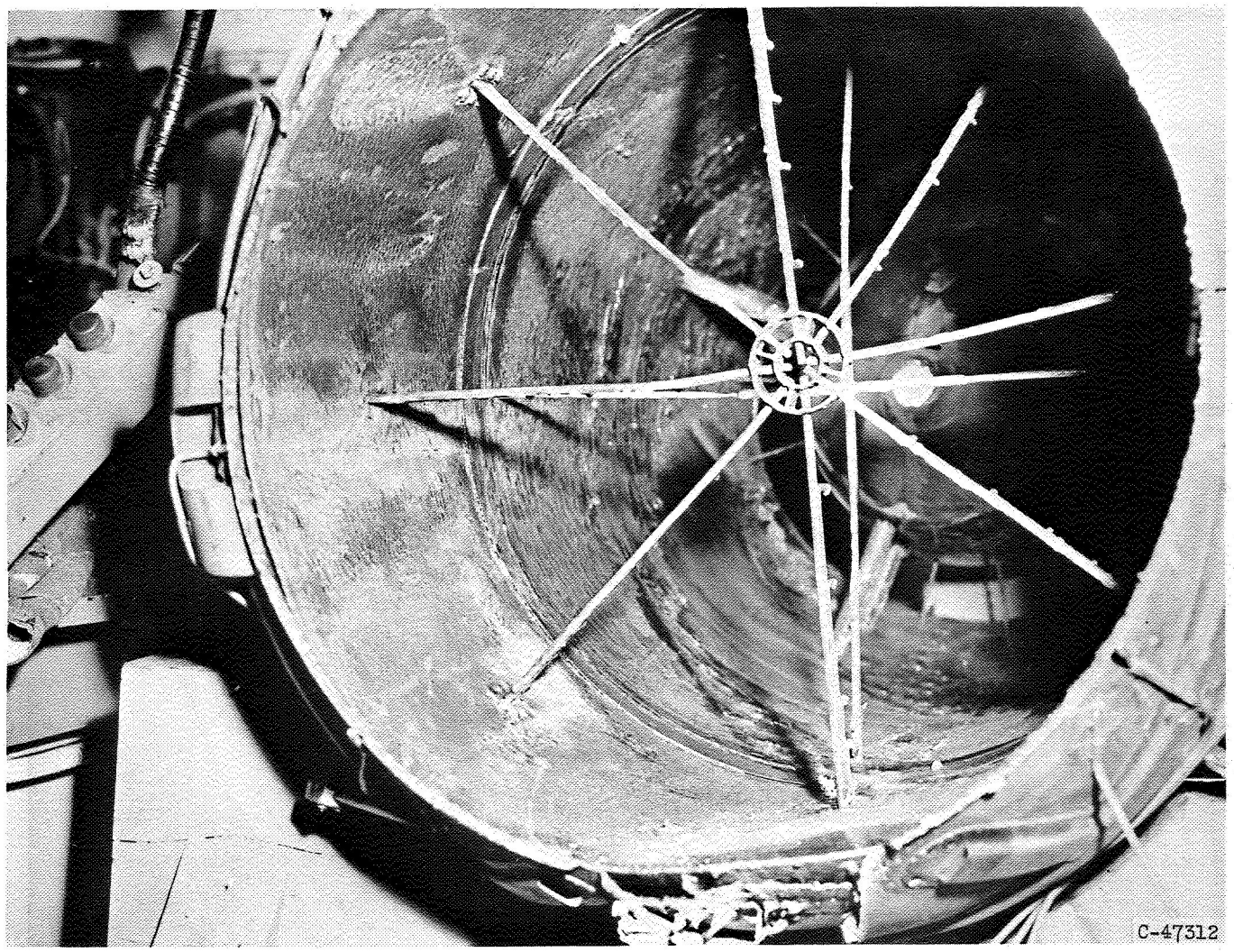

(b) Tailpipe and exhaust nozzle, pentaborane run.

Figure 9. - Continued. Oxide deposits on tailpipe diffuser, tailpipe, and exhaust nozzle

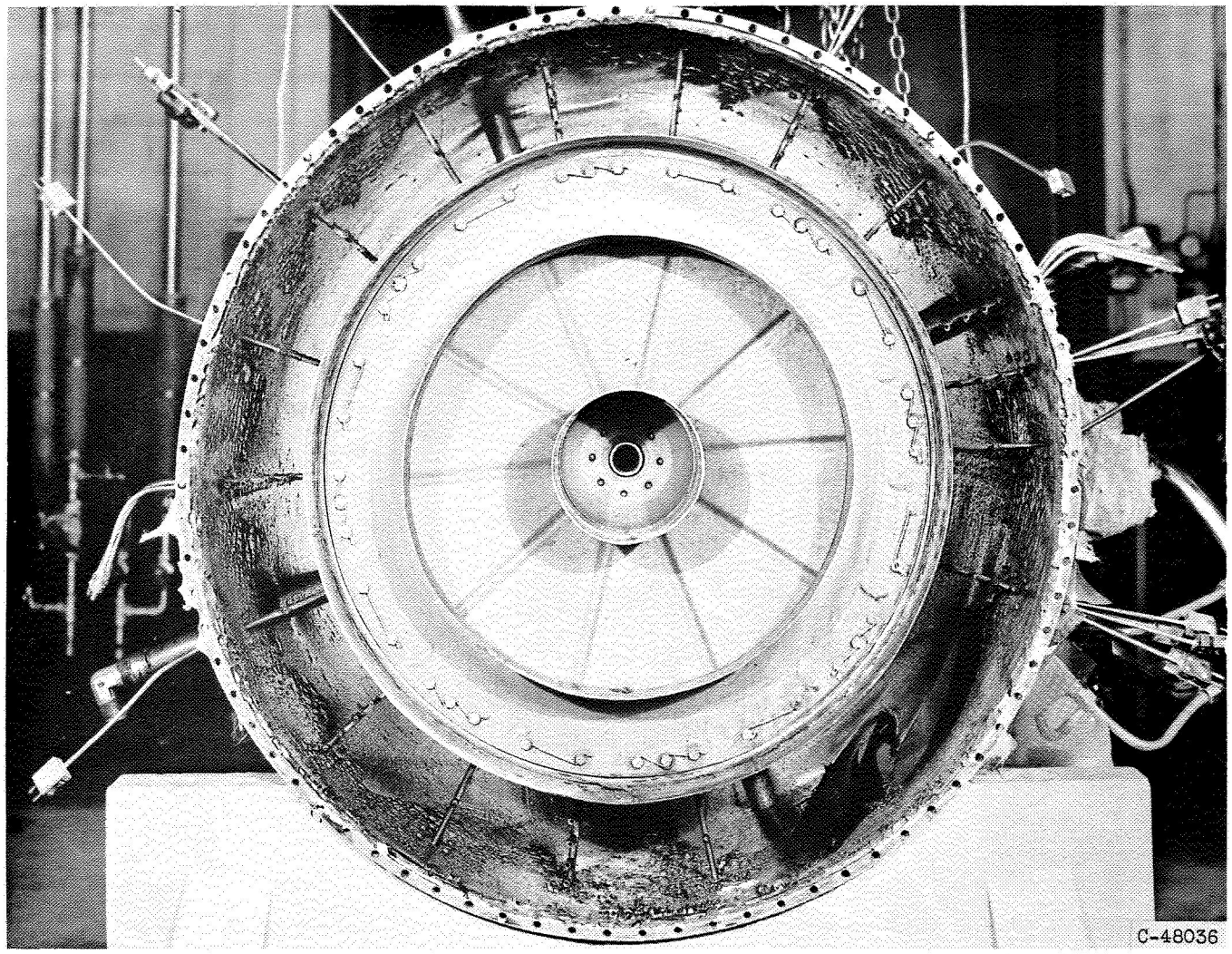

(c) Tailpipe, HEF-2 run.

Figure 9. - Continued. Oxide deposits on tailpipe diffuser, tailpipe, and exhaust nozzle.

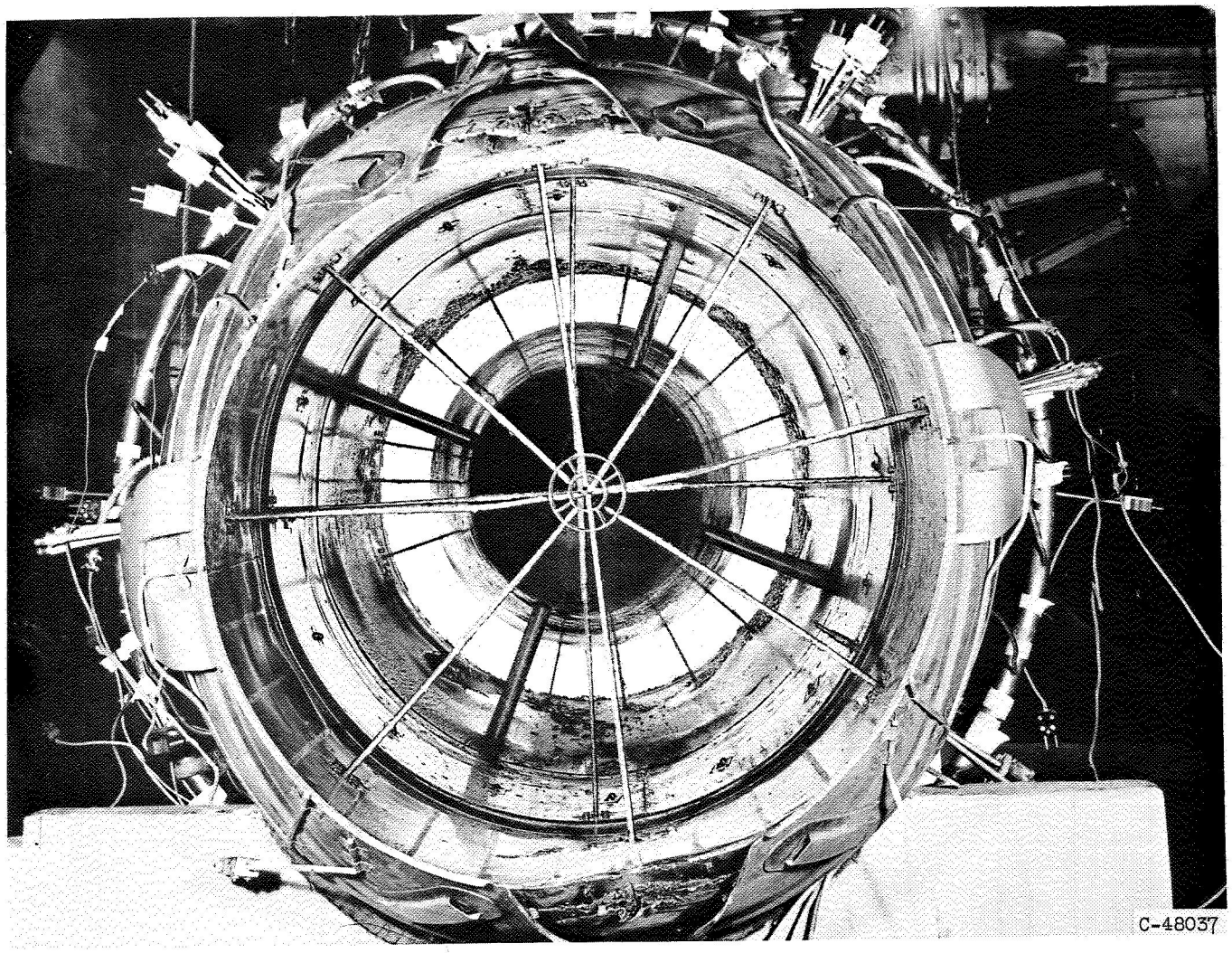

(a) Tailpipe and le, ·2 run.

Fi 9. Concluded. Oxi e ts on tailpipe diffuser, a le.

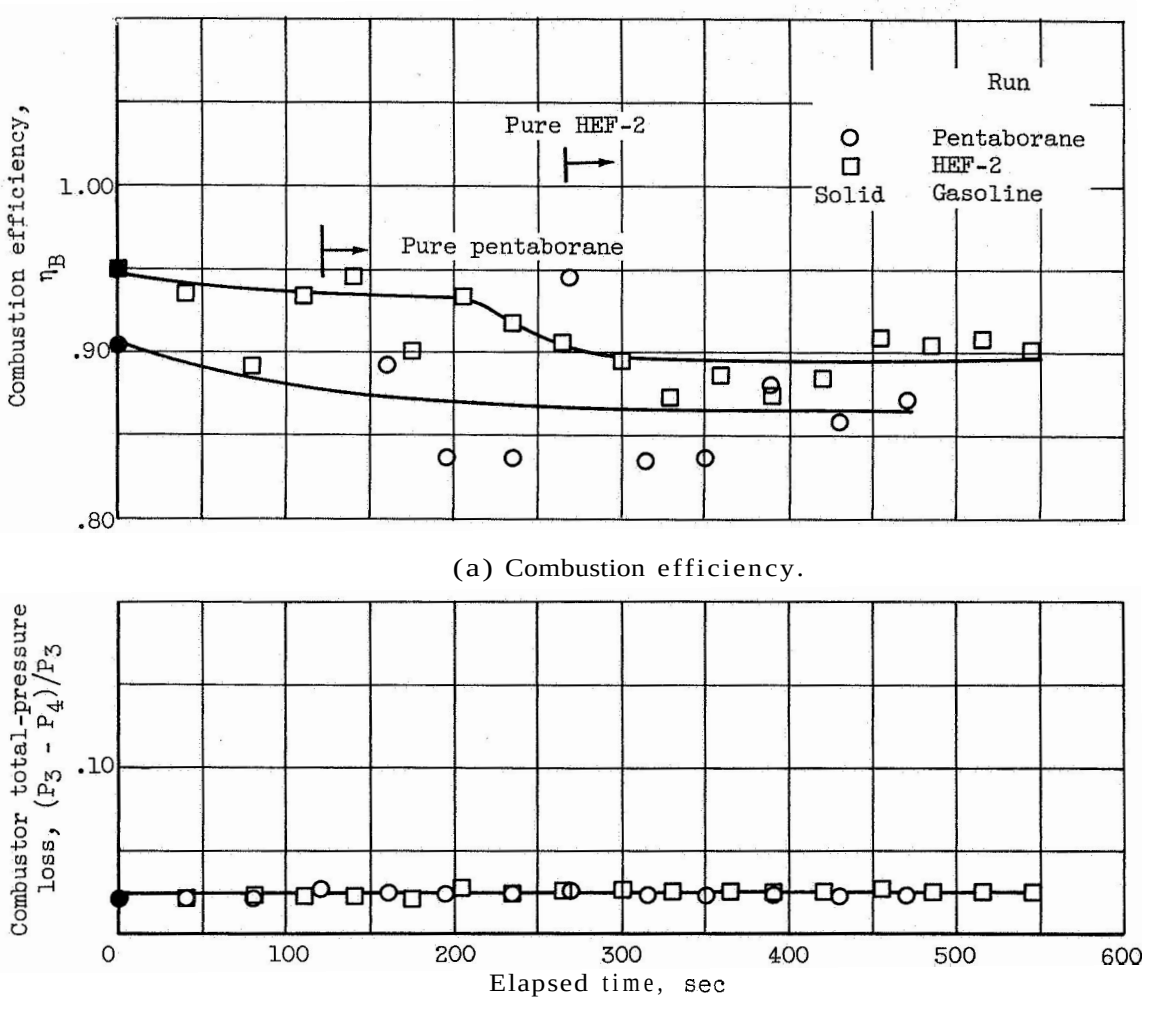

(a) Combustion efficiency.

(b) Combustor total-pressure loss.

Figure 10. - Effect of operation with pentaborane fuel and HEF-2 on combustor performance.

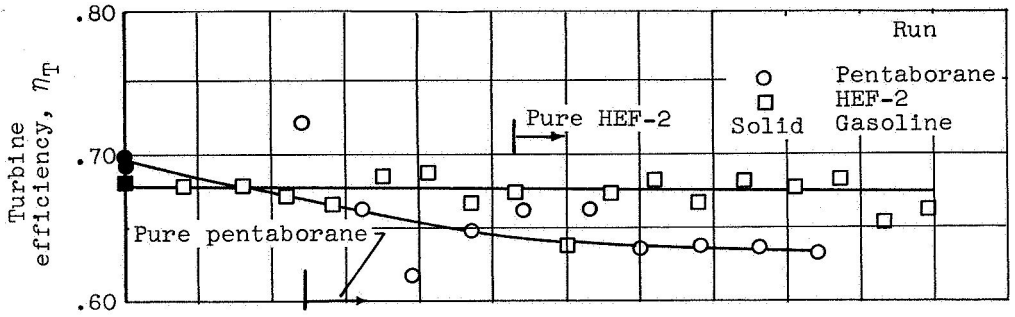

(a) Turbine efficiency.

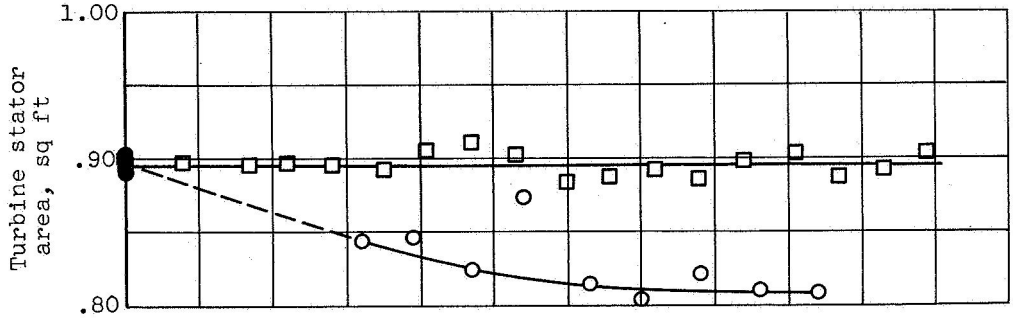

(b) Turbine stator area.

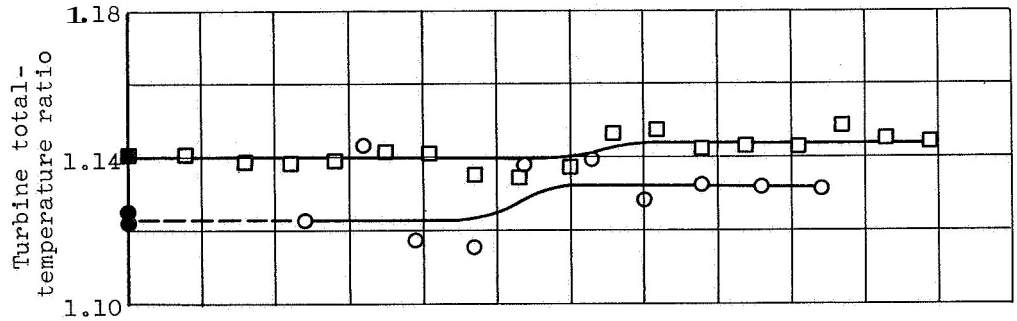

(c) Turbine total-temperature ratio.

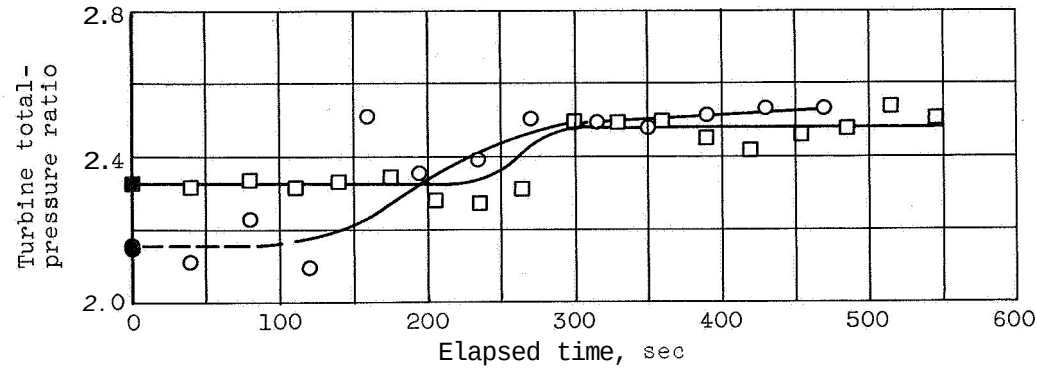

(d) Turbine total-pressure ratio.

Figure 11. - Effect of operation with pentaborane fuel and HEF-2 on turbine performance.

E-118

CE-5 back

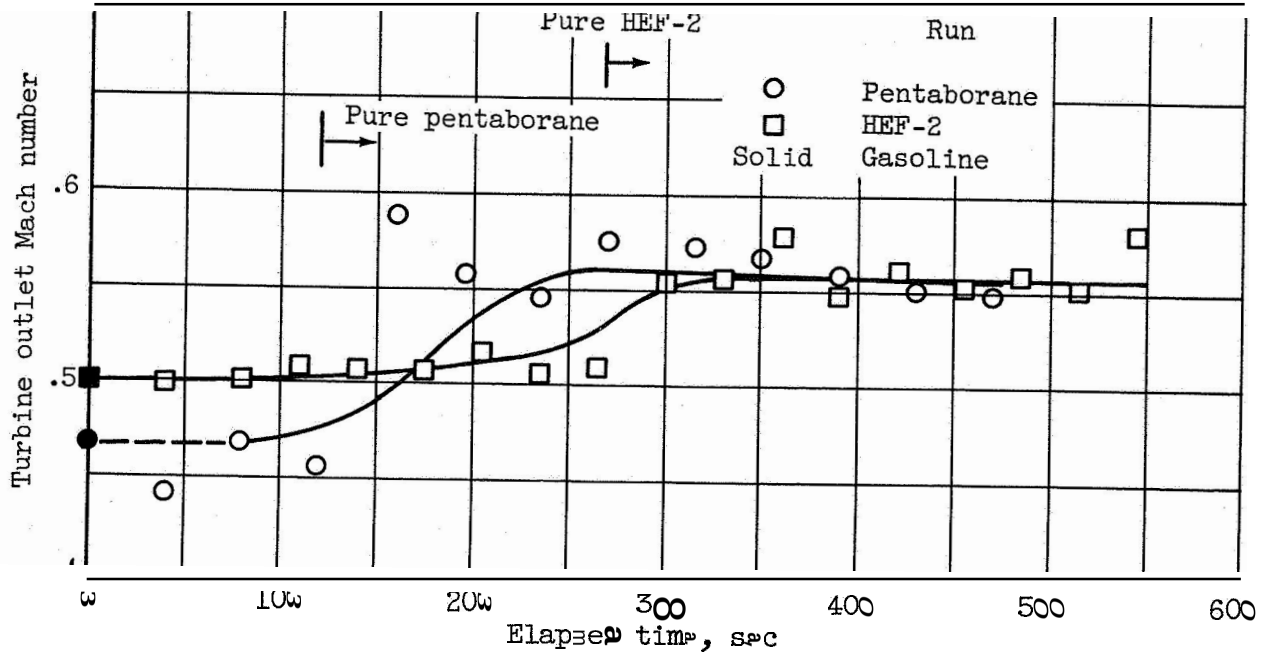

Figure 12. - Variation of turbine outlet Mach number during operation with pentaborane fuel and HEF-2.

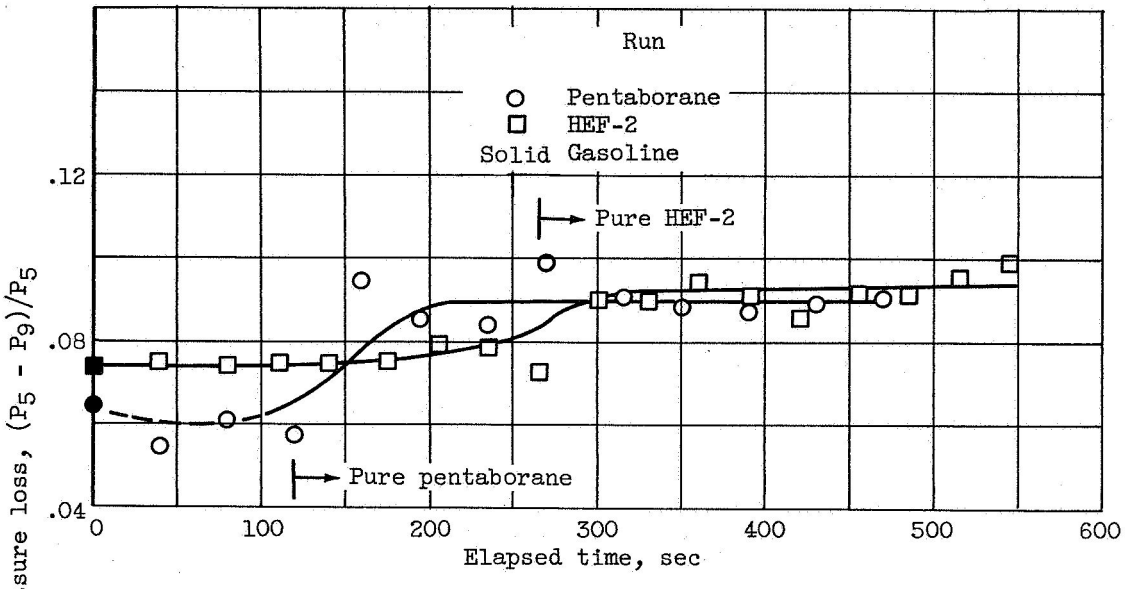

(a) Effect of time.

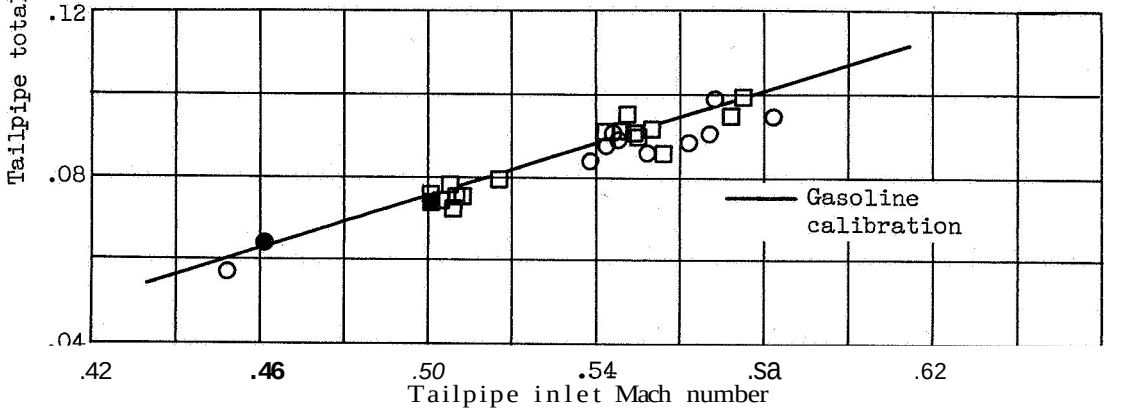

(b) Effect of tailpipe inlet Mach number.

Figure 13. - Effect of operation with pentaborane fuel and HEF-2 on tailpipe performance.

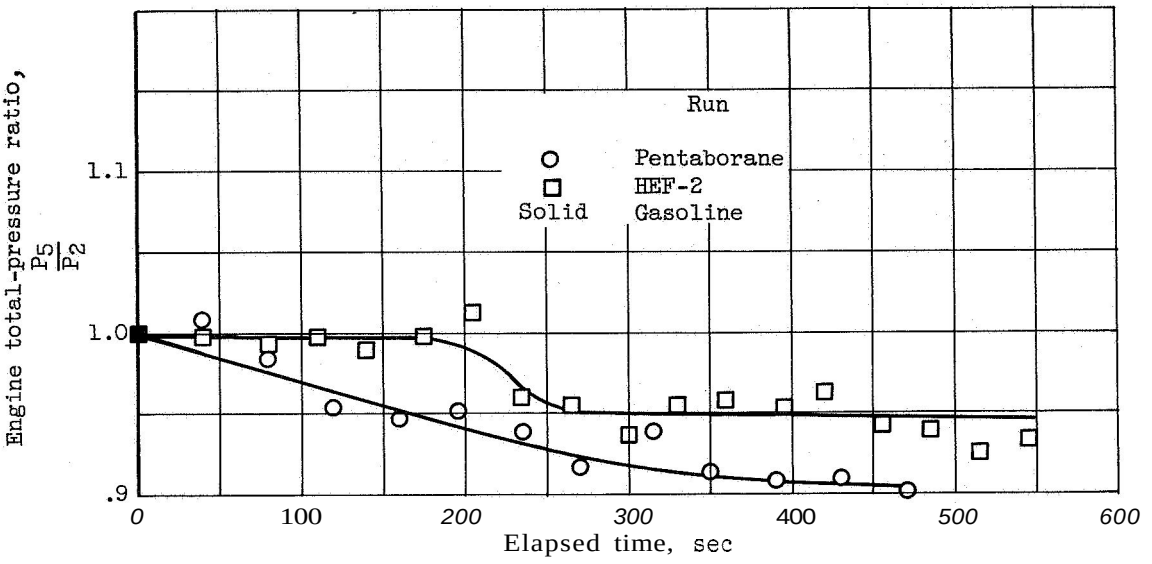

Figure 14. - Effect of operation with pentaborane fuel and HEF-2 on engine total-pressure ratio.

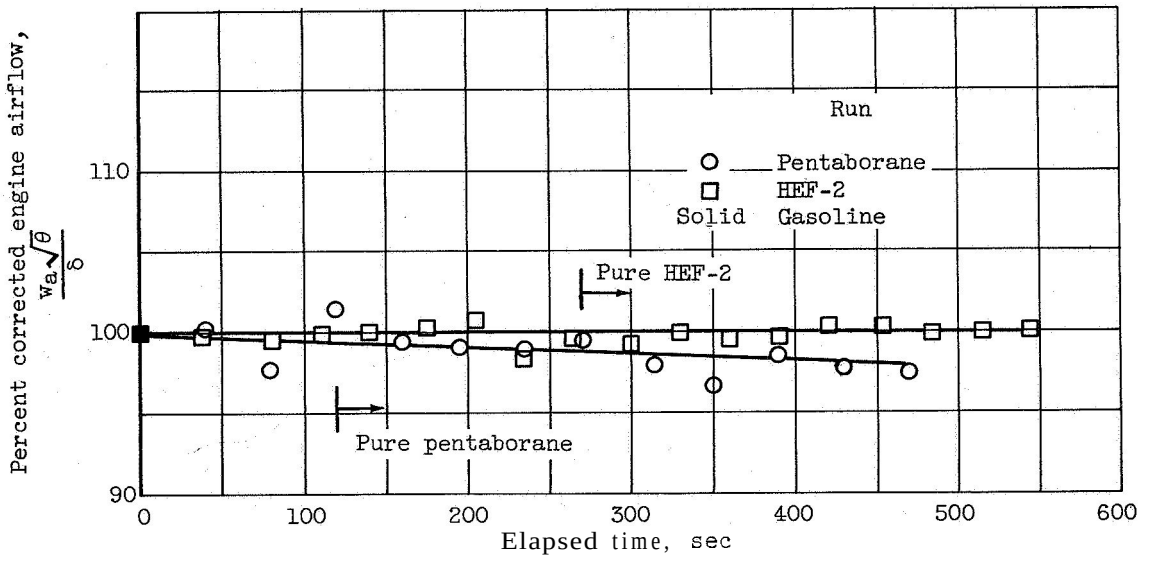

Figure 15. - Effect of operation with pentaborane fuel and HEF-2 on engine corrected airflow.

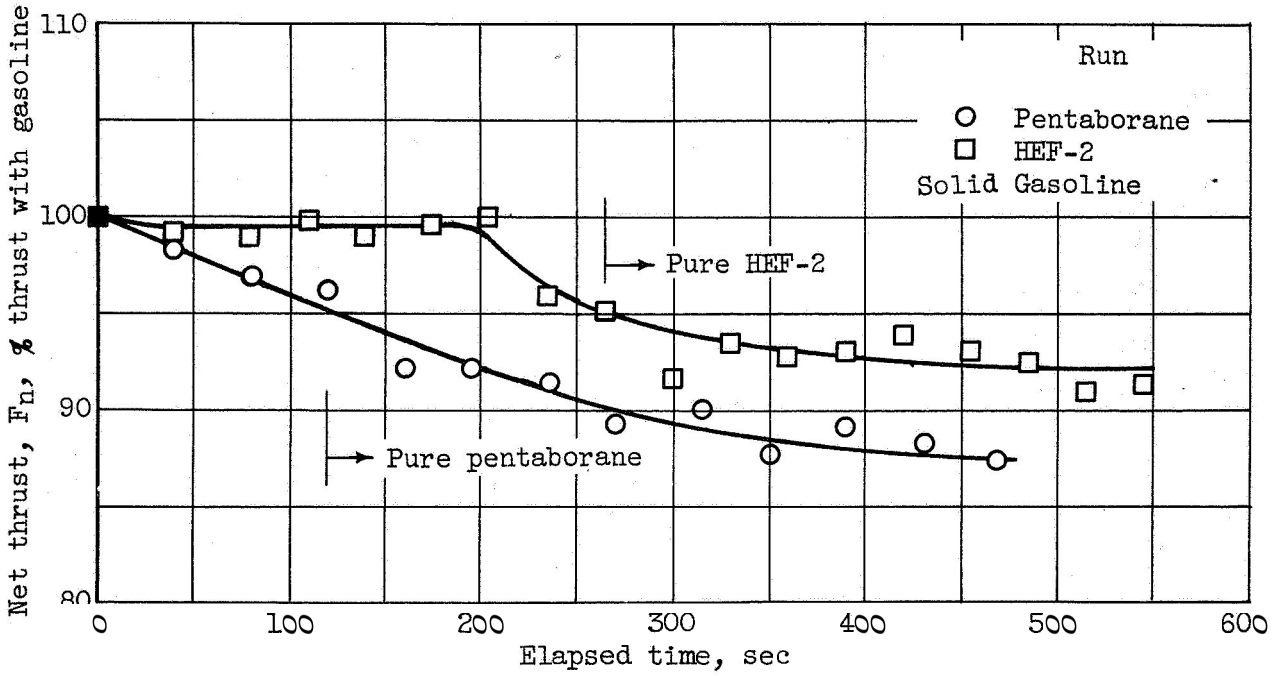

(a) Comparison of net thrusts

Figure 16. - Effect of operation with pentaborane fuel and HEF-2 on net thrust.

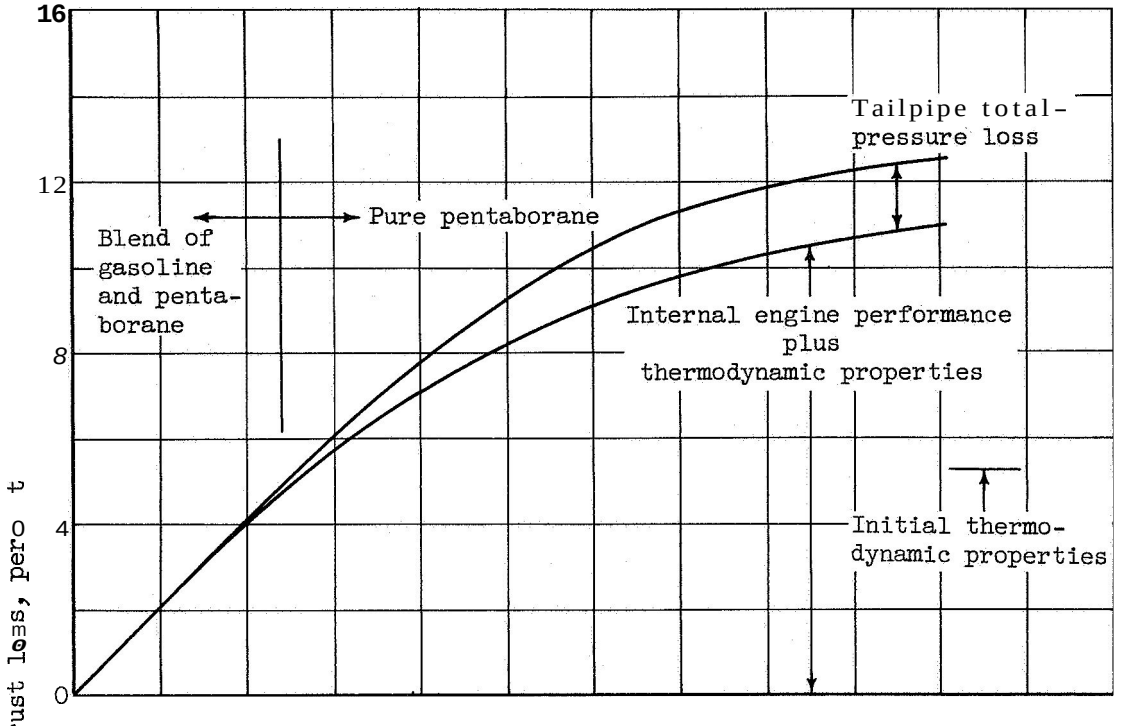

(b) Thrust-loss breakdown for pentaborane fuel fun.

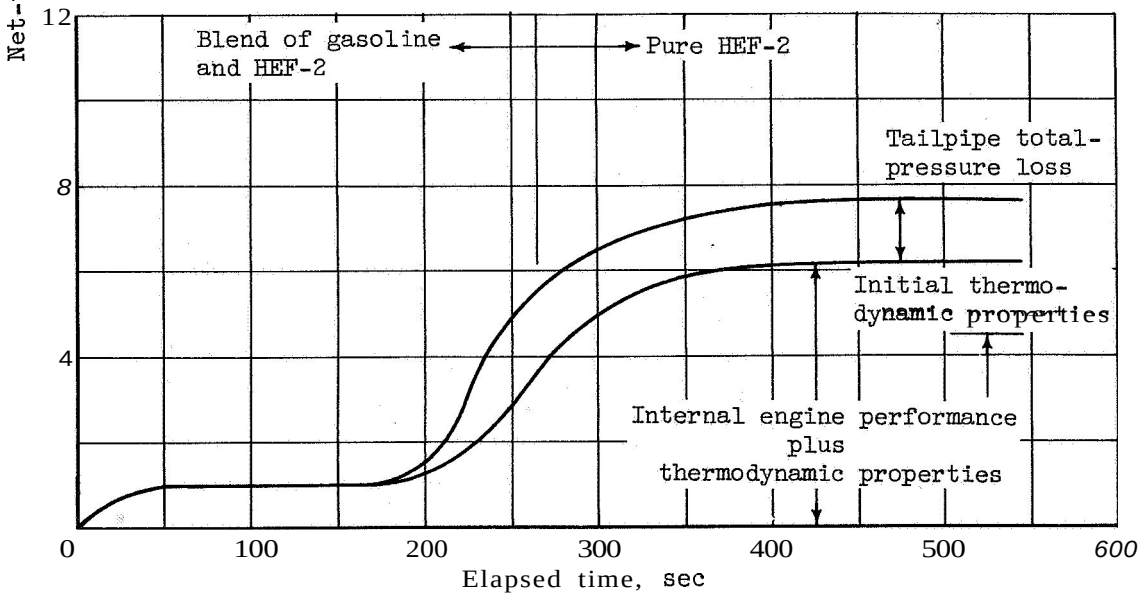

(c) Thrust-loss breakdown for REF-2 run.

Figure 16. - Concluded. Effect of operation with pentaborane fuel and HEF-2 on net thrust.